

Title: A population of adult satellite-like cells in *Drosophila* is maintained through a switch in RNA-isoforms

Authors: Hadi Boukhatmi and Sarah Bray*

Department of Physiology Development and Neuroscience,
University of Cambridge
Downing Street
Cambridge, CB2 3DY, UK

*corresponding author: sjb32@cam.ac.uk

Summary

Adult stem cells are important for tissue maintenance and repair. One key question is how such cells are specified and then protected from differentiation for a prolonged period. Investigating the maintenance of *Drosophila* muscle progenitors (MPs) we demonstrate that it involves a switch in *zfh1/ZEB1* RNA-isoforms. Differentiation into functional muscles is accompanied by expression of *miR-8/miR-200*, which targets the major *zfh1-long* RNA isoform and decreases Zfh1 protein. Through activity of the Notch pathway, a subset of MPs produce an alternate *zfh1-short* isoform, which lacks the *miR-8* seed site. Zfh1 protein is thus maintained in these cells, enabling them to escape differentiation and persist as MPs in the adult. There, like mammalian satellite cells, they contribute to muscle homeostasis. Such preferential regulation of a specific RNA isoform, with differential sensitivity to miRs, is a powerful mechanism for maintaining a population of poised progenitors and may be of widespread significance.

1 INTRODUCTION

2 Growth and regeneration of adult tissues depends on stem cells, which remain
3 undifferentiated while retaining the potential to generate differentiated progeny. For
4 example, muscle satellite cells (SCs) are a self-renewing population that provides the
5 myogenic cells responsible for postnatal muscle growth and muscle repair (Chang and
6 Rudnicki, 2014). One key question is how tissue specific stem cells, such as satellite cells,
7 are able to escape from differentiation and remain undifferentiated during development, to
8 retain their stem cell programme though-out the lifetime of the animal.

9 It has been argued that the progenitors of *Drosophila* adult muscles share similarities with
10 satellite cells and thus provide a valuable model to investigate mechanisms that maintain
11 stem cell capabilities (Aradhya, et al., 2015; Figeac, et al., 2007). After their specification
12 during embryogenesis, these muscle progenitors (MPs) remain undifferentiated throughout
13 larval life before differentiating during pupal stages. For example, one population of MPs is
14 associated with the wing imaginal disc, which acts as a transient niche, and will ultimately
15 contribute to the adult flight muscles. These MPs initially divide symmetrically to amplify
16 the population. They then enter an asymmetric division mode in which they self-renew and
17 generate large numbers of myoblasts that go on to form the adult muscles (Gunage, et al.,
18 2014). In common with vertebrates, activity of Notch pathway is important to maintain the
19 MPs in an undifferentiated state (Gunage, et al., 2014; Mourikis and Tajbakhsh, 2014;
20 Mourikis, et al., 2012; Bernard, et al., 2010). To subsequently trigger the muscle
21 differentiation program, levels of Myocyte Enhancer factor 2 (Mef2) are increased and
22 Notch signalling is terminated (Elgar, et al., 2008; Bernard, et al., 2006). Until now it was
23 thought that all MPs followed the same fate, differentiating into functional muscles.
24 However, it now appears that a subset persist into adulthood forming a population
25 satellite-like cells ((Chaturvedi, et al., 2017) and see below). This implies a mechanism
26 that enables these cells to escape from differentiation, so that they retain their progenitor-
27 cell properties.

28 The *Drosophila* homologue of ZEB1/ZEB2, ZFH1 (zinc-finger homeodomain 1), is a
29 candidate for regulating the MPs because this family of transcription factors is known to
30 repress Mef2, to counteract the myogenic programme (Postigo and Dean, 1999; Postigo,
31 et al., 1999). Furthermore, *zfh1* is expressed in the MPs when they are specified in the
32 embryo and was shown to be up-regulated by Notch activity in an MP-like cell line (DmD8)

33 (Figeac, et al., 2010; Krejci, et al., 2009). Furthermore, an important regulatory link has
34 been established whereby microRNAs (miRs) are responsible for down-regulating
35 ZEB/Zfh1 protein expression to promote differentiation or prevent metastasis in certain
36 contexts (Zaravinos, 2015; Vandewalle, et al., 2009). For example, the miR-200 family is
37 significantly up-regulated during type II cell differentiation in fetal lungs, where it
38 antagonizes ZEB1 (Benlhabib, et al., 2015). Likewise, *miR-8*, a *miR-200* relative,
39 promotes timely terminal differentiation in progeny of *Drosophila* intestinal stem cells by
40 antagonizing *zfh1* and *escargot* (Antonello, et al., 2015). Conversely, down-regulation of
41 *miR-200* drives epithelial mesenchymal transition (EMT) to promote metastasis in multiple
42 epithelial derived tumours (Korpala, et al., 2008; Park, et al., 2008). Such observations
43 have led to the proposal that the ZEB/miR-200 regulatory loop may be important in the
44 maintenance of stemness, although examples are primarily limited to cancer contexts and
45 others argue that the primary role is in regulating EMT (Antonello, et al., 2015; Brabletz
46 and Brabletz, 2010). The MPs are thus an interesting system to investigate whether this
47 regulatory loop is a gatekeeper for the stem cell commitment to differentiation.

48 To investigate the concept that ZEB1/Zfh1 could be important in sustaining progenitor-type
49 status, we examined the role and regulation of *zfh1* in *Drosophila* MPs/SCs. Our results
50 show that *zfh1* plays a central role in the maintenance of undifferentiated MPs and,
51 importantly, that its expression is sustained in a population of progenitors that persist in
52 adults (pMPs). Specifically these pMPs express an alternate short RNA isoform of *zfh1*
53 that cannot be targeted by *miR-8*. In contrast, the majority of larval precursors express a
54 long isoform of *zfh1*, which is subject to regulation by *miR-8* so that Zfh-1 protein levels are
55 suppressed to enable differentiation of myocytes. Expression of alternate *zfh1-short*
56 isoform is thus a critical part of the regulatory switch to maintain a pool of progenitor
57 “satellite-like” cells in the adult. This type of regulatory logic, utilizing RNA isoforms with
58 differential sensitivity to miRs, may be of widespread relevance for adult stem cell
59 maintenance in other tissues.

60

61 RESULTS

62

63 **Zfh1 is required for maintenance of muscle progenitors**

64 As *zfh1* was previously shown to antagonize myogenesis it was a plausible candidate to
65 maintain the muscle progenitor cells in *Drosophila* and prevent their differentiation. We
66 therefore examined its expression in the muscle progenitors (MPs) associated with the
67 wing disc. Zfh1 was clearly present throughout the large group of MPs, which can be
68 distinguished by the expression of Cut (Ct) (Figure 1A-A''). At early stages Zfh1 is
69 uniformly expressed throughout the MPs (Figure supplement 1) but at later stages the
70 levels become reduced in the cells with high Cut expression (Figure 1 A''). These cells
71 give rise to the direct flight muscles (DFMs), whereas the remaining MPs, where Zfh1
72 expression is high, give rise to the indirect flight muscles (IFMs) (Figure 1 A''; (Sudarsan,
73 et al., 2001)). Zfh1 expression in MPs is therefore regulated in a manner that correlates
74 with different differentiation programmes.

75 To determine whether Zfh1 is required in the MPs to antagonize myogenic differentiation
76 we tested the consequences from expressing a hairpin RNA to target/silence *zfh1*
77 *specifically* in MPs (using *1151-Gal4* as a driver). Tropomyosin (Tm), a protein normally
78 expressed in differentiated muscles, was clearly detectable when *zfh1*-was down-
79 regulated (Figure 1B-C). A similar result was obtained using a Myosin Heavy Chain (MHC)
80 reporter, which revealed that small muscle fibers formed precociously in ~ 20% of *zfh-1*
81 depleted wing discs (n=4/20 wing discs; Figure supplement 1). Consistent with the
82 premature expression of muscle differentiation markers, β -3Tubulin staining showed that
83 decreased *zfh1* led to abnormal MP cell morphology (Figure 1B'-C'). These results
84 demonstrate that reduced *zfh1* expression causes MPs to initiate the muscle differentiation
85 program indicating that *zfh1* is required to prevent MP differentiation.

86 Lineage tracing experiments suggest that a subset of wing disc MPs have characteristics
87 of muscle stem cells and remain undifferentiated even in adult *Drosophila* (Chaturvedi, et
88 al., 2017; Gunage, et al., 2014). Since Zfh-1 is necessary to prevent differentiation in MPs,
89 we reasoned that its expression might be sustained in these persistent muscle progenitors
90 (pMPs). Indeed, some individual cells, closely associated with adult IFM muscle fibers,
91 had high levels of Zfh1 expression whereas the differentiated muscle nuclei exhibited no
92 detectable expression (Figure 1D-D'). To better characterise these Zfh1-positive adult cells,

93 we expressed a membrane-tagged GFP (*UAS-Src::GFP*) under the control of a specific
94 muscle driver *mef2-Gal4* (*mef2>GFP*). This confirmed that *Zfh1* was expressed in
95 *mef2>GFP* expressing cells, indicating they were myogenic, and that these cells were
96 closely embedded in the muscle lamina (Figure 1E-E’’). These cells therefore have
97 characteristics of persistent muscle progenitors and likely correspond to the so-called adult
98 satellite cells recently identified by others (Figure 1D and E). Although many of the *Zfh1*
99 expressing cells were clearly co-expressing *Mef2>GFP*, *Zfh1* was also detected in another
100 population that lacked *Mef2* expression. Often clustered, these cells were co-labelled with
101 a plasmatocyte marker *P1/Nimrod* indicating that they are phagocytic immune cells (Figure
102 supplement 2).

103 The results demonstrate that *Zfh1* is expressed in MPs, where it is required for their
104 maintenance, and that its expression continues into adult-hood in a small subset of
105 myogenic cells. If, as these data suggest, *Zfh1* is important for sustaining a population of
106 a persistent adult progenitors, there must be a mechanism that maintains *Zfh1* expression
107 in these cells while the remainder differentiate into functional flight muscles.

108

109 ***zfh1* enhancers conferring expression in MPs**

110 To investigate whether the maintenance of *Zfh1* expression in larval and adult MPs could
111 be attributed to distinct enhancers, we screened *enhancer-Gal4* collections (Jenett, et al.,
112 2012; Jory, et al., 2012; Manning, et al., 2012) to identify *zfh1* enhancers that were active
113 in larval MPs. From the fifteen enhancers across the *zfh1* genomic locus that were tested,
114 (Figure 2 and Figure supplement 3 A) three directed GFP expression in the *Cut* expressing
115 MPs (Figure 2B-D). These all correlated with regions bound by the myogenic factor *Twist*
116 in muscle progenitor related cells (Figure supplement 3 A and (Bernard, et al., 2010)).
117 Enhancer 1 (*Enh1*; VT050105) conferred weak expression in scattered progenitors (Figure
118 2B). Enhancer 2 (*Enh2*; VT050115) was uniformly active in all MPs and also showed
119 ectopic expression in some non-*Cut* expressing cells (Figure 2C). Finally, Enhancer 3
120 (*Enh3*; GMR35H09) conferred expression in several MPs with highest levels in a subset
121 located in the posterior (Figure 2D). *Enh3* encompasses a region that was previously
122 shown to be bound by *Su(H)* in muscle progenitor related cells, hence may be regulated
123 by Notch activity (Figure supplement 3A; (Bernard, et al., 2010; Krejci, et al., 2009). These
124 results demonstrate that several enhancers contribute to *zfh1* expression in the MPs.

125 To determine which enhancer(s) are also capable of conferring *zfh-1* expression in adult
126 pMPs we assessed their activity in adult muscle preparations. Only Enh3 exhibited any
127 activity in these cells (Figure 2E), where it recapitulated well Zfh1 protein expression
128 (Figure 2 E-E’). Thus, Enh3-GFP was clearly detectable in scattered cells, which were
129 closely apposed to the muscle fibers and contained low levels of Mef-2 (Figure 2E’), and
130 was not expressed in the differentiated muscle nuclei (Figure 2). These results suggest
131 that Enh3 is responsible for maintaining *zfh1* transcription in the adult pMPs.

132 If Enh3 is indeed necessary for expression of *zfh1* in MPs and pMPs, its removal should
133 curtail *zfh1* expression in those cells. To test this, Enh3 was deleted by Crispr/Cas9
134 genome editing (Δ Enh3; see material and methods). Δ Enh3 homozygous flies survived
135 until early pupal stages allowing us to analyze the phenotype at larval stages. As predicted,
136 Δ Enh3 MPs exhibited greatly reduced Zfh1 protein expression (Figure 3F-H) that
137 correlated with decreased *zfh1* mRNA levels (Figure supplement 3B). Although striking,
138 the effects of Δ Enh3 did not phenocopy those of depleting *zfh1* using RNAi, as no
139 premature up-regulation of muscle differentiation markers (MHC, Tm) occurred in Δ Enh3
140 discs (data not shown). This is likely due to residual *zfh1* mRNA/protein (Figure 2G),
141 brought about by the activity of other *zfh1* enhancers (e.g. Enh1 and Enh2, Figure 2B-C).
142 Nevertheless, it is evident that Enh3 has a key role in directing *zfh1* expression in MPs.

143

144 **Adult Zfh1+ve MP cells contribute to flight muscles**

145 By recapitulating Zfh1 in adult MPs, Enh3 provides a powerful tool to investigate whether
146 the persistent MPs are analogous to muscle satellite cells, which are able to divide and
147 produce committed post-mitotic myogenic cells that participate in muscle growth and
148 regeneration. To address this we used a genetic G-trace method, which involves two UAS
149 reporters, an RFP reporter that directly monitors the current activity of the Gal4 and a GFP
150 reporter that records the history of its expression to reveal the lineage (Evans, et al., 2009).
151 When *Enh3-Gal4* was combined with the G-trace cassette RFP expression was present in
152 the muscle-associated pMPs, which have low Mef2 expression (Figure 2I-I’). Strikingly,
153 most of the muscle nuclei expressed GFP (Figure 2I’-I’’) suggesting that they are derived
154 from ancestral Enh3 expressing cells (Figure 2I’). Furthermore, close examination of the
155 Enh3 driven RFP expression showed that it often persisted in two nearby muscle nuclei.
156 This suggests that these nuclei are recent progeny of Enh3 expressing cells, indicating
157 that these cells have kept the ability to divide that is characteristic of a satellite-like stem

158 cell population (Figure 2). To further substantiate this conclusion, we verified that adult
159 Zfh1+ve cells were actively dividing cells, using the mitotic marker phosphohistone-3
160 (PH3) staining. Many examples of Zfh1+ve cells co-stained for PH3 (Figure 2J-J'')
161 indicating that these adult cells are dividing cells. Taken together the results argue that the
162 adult Zfh1+ve cells resemble mammalian satellite cells, retaining the capacity to divide and
163 provide progeny that maintain the adult flight muscles.

164 **Notch directly regulates *zfh1* expression in muscle progenitors and adults pMPs**

165 As mentioned above, *zfh1* is regulated by Notch activity in *Drosophila* DmD8, MP-related,
166 cells (Krejci, et al., 2009), where Enh3 was bound by Su(H) (Figure 2A and Figure
167 supplement 3). Furthermore, phenotypes from depletion of *zfh1* in MPs, were reminiscent
168 of those elicited by loss of Notch (N) signaling (Figure 1 and (Krejci, et al., 2009)). Notch
169 activity is therefore a candidate to maintain Zfh1 expression in the adult pMPs, thereby
170 preventing their premature differentiation. As a first step to test whether Notch activity
171 contributes to *zfh1* expression, we depleted *Notch* in muscle progenitors by driving Notch
172 RNAi expression with *1151-Gal4* (Figure 3A-B and C). Under these conditions, Zfh1
173 expression was significantly reduced consistent with Notch being required for *zfh1*
174 expression in MPs. Second, the consequences of perturbing Notch regulation by mutating
175 the Su(H) binding motifs in Enh3 were analyzed. Two potential Su(H) binding sites are
176 present in Enh3 and both are highly conserved across species (Figure 2A). Mutation of
177 both motifs, *Enh3[mut]*, resulted in a dramatic decrease of the enhancer activity in the MPs
178 (Figure 3D-E and F). This supports the hypothesis that Notch directly controls *zfh1*
179 expression in MPs by regulating activity of Enh3.

180 Since Enh3 activity persists in the adult MPs (Figure 2), we next analyzed whether
181 mutating the Su(H) motifs impacted expression in these adult pMPs. Similar to larval
182 stage MPs, *Enh3[mut]* had lost the ability to direct expression of GFP in the adult pMPs
183 (Figure 3G-H). Thus, the Su(H) motifs are essential for Enh3 to be active in the adult pMPs.
184 These data support the model that persistence of Zfh1 expression in adult MPs is likely
185 due to Notch input, acting throughout Enh3.

186 The results imply that Notch should be expressed and active in the adult pMPs. To
187 investigate this, we made use of a *Notch[NRE]-GFP* reporter line. *Notch[NRE]* is an
188 enhancer from the *Notch* gene, and itself regulated by Notch activity, such that it is a read
189 out both of Notch expression and of Notch activity (Simon, et al., 2014). Strikingly,
190 *Notch[NRE]-GFP* reporter is consistently expressed in the Zfh1+ve adult pMPs, confirming

191 that Notch is active in these cells (Figure 3I) but not in the differentiated muscles. It is also
192 active in some surrounding non-muscles cells/tissues (Figure 3I). Together, the results
193 show that *zfh1* expression in the adult pMPs requires Notch activity acting through Enh3.

194 ***zfh1* is silenced by the conserved microRNA *miR-8/miR-200* in MPs**

195 Although transcriptional control of *zfh1* by Notch explains one aspect of its regulation,
196 since all larval MPs express Zfh1 it remained unclear how a subset maintain this
197 expression and escape from differentiation to give rise to the adult pMPs. A candidate to
198 confer an additional level of regulation on *zfh1* expression is *miR-8/miR-200*, which is
199 important for silencing *zfh1* (and its mammalian homologue ZEB1) in several contexts. The
200 regulatory loop between *miR-8/miR-200* and *zfh1/ZEB* has been extensively studied in
201 both *Drosophila* and vertebrates and is mediated by a *miR-8/miR-200* seed site located in
202 the 3' untranslated region (3'UTR) (Antonello, et al., 2015; Vallejo, et al., 2011; Brabletz
203 and Brabletz, 2010).

204 To determine whether *miR-8* could down-regulate *zfh1* in muscle progenitors to promote
205 their differentiation into muscles, we first examined the spatiotemporal expression pattern
206 of *miR-8* at larval and adult stages (Figure 4) using *miR-8-Gal4*, whose activity reflects the
207 expression of the endogenous *miR-8* promoter (Karres, et al., 2007). *miR-8-Gal4* was
208 combined with a membrane GFP (for Progenitors, Figure 4A) or a nuclear GFP (for Adult
209 muscles nuclei, Figure 4D) to visualize its expression. At larval stages, *miR-8* expression
210 was inversely correlated with Zfh1 levels. Thus in most of the MPs, where Zfh1
211 expression was high, there was little or no expression from *miR-8-Gal4* (Figure 4 B-B' and
212 Figure 1A). Conversely, in the subset of MPs where Zfh1 is low (high Ct expressing DFM
213 precursors) there were correspondingly higher levels of *miR-8-Gal4*, although the absolute
214 levels were low compared to some of the surrounding tissues; Figure 4C-C' and Figure 1
215 A). In contrast, adult muscles had uniform and high levels of *miR-8-Gal4*; all of the
216 differentiated muscle nuclei exhibited nuclear GFP (Figure 4D-D'). Strikingly, at the same
217 time, *miR-8-Gal4* expression was absent from the Zfh1+ve adult pMPs (Figure 4D-D').
218 These data show that, during muscle formation, *miR-8* and Zfh1 are expressed in a
219 mutually exclusive manner; supporting the model that *miR-8* negatively regulates *zfh1*.

220 To further address this regulation, we tested the impact of *miR-8* overexpression on Zfh1
221 protein levels in MPs at larval stage (Figure 4). Zfh1 protein levels were significantly
222 diminished under these conditions, in agreement with *miR-8* regulating *zfh1* post-
223 transcriptionally (Figure 4E-G). Although this manipulation was not sufficient to cause

224 premature up-regulation of muscle differentiation markers, the few surviving adults all
225 displayed a held-out wing phenotype, which is often associated with defective flight
226 muscles (Vigoreaux, 2001).

227 Next we assessed whether *miR-8* activity/expression changes in response to Mef2 levels,
228 a critical determinant of muscle differentiation, using a *miR-8* sensor (containing two *miR-8*
229 binding sites in its 3'UTR (Kennell, et al., 2012). Expression of the *miR-8* sensor was
230 specifically decreased when Mef2 was overexpressed in MPs, suggesting that *miR-8*
231 expression responds to high level of Mef2 (Figure supplement 4). Together, these data
232 argue that *miR-8* up-regulation during muscle differentiation blocks Zfh1 production to
233 allow MPs to differentiate.

234

235 **An alternate short *zfh1* isoform is transcribed in adult MPs**

236 To retain their undifferentiated state, the adult pMPs must evade *miR-8* regulation and
237 maintain Zfh1 expression. The *zfh1* gene gives rise to three different mRNA isoforms; two
238 long *zfh1* isoforms (*zfh1-long*; *zfh1-RE/RB*) and one short *zfh1* isoform (*zfh1-short*; *zfh1-*
239 *RA*) (Figure 5A). Although long *zfh1* isoforms have two additional N-terminal zinc fingers,
240 all three RNA-isoforms produce proteins containing the core zinc finger and
241 homeodomains needed for Zfh1 DNA-binding activity (Figure supplement 5; (Postigo, et
242 al., 1999)). Importantly, *zfh1-short* isoform has a shorter 3'UTR, which lacks the target site
243 for *miR-8* (Figure 5A; (Antonello, et al., 2015), as well as differing in its transcription start
244 site (TSS) (Figure 5A; Flybase FBgn0004606). As *zfh1-short* is predicted to escape *miR-8*
245 mediated down-regulation, its expression will enable cells to retain high level of Zfh1
246 protein, explaining how the adult pMPs can escape differentiation. To test this prediction,
247 we designed fluorescent probes specific for the *zfh1-long* and *zfh1-short* isoforms and
248 used them for in situ hybridization (FISH) at larval and adult stages (Figure 5A). In the
249 larval stage (L3), *zfh1-long isoforms were* present at uniformly high levels in the MPs
250 (Figure 5B-B'") whereas *zfh1-short* was expressed at much lower levels and only detected
251 in a few MPs in each disc (Figure 5C-C'").

252 We then analyzed *zfh1* isoforms expression in adult muscles, where the adult pMPs were
253 marked by *Enh3-Gal4>GFP* and low Mef2 expression (Figure 5D-E). In contrast to MPs in
254 the larva, these adult pMPs expressed high levels of *zfh1-short* and much lower levels of
255 *zfh1-long* (Figure 5D-E'"). *zfh1-short* was only present in the pMPs whereas dots of *zfh1-*
256 *long* hybridization were also detected in some differentiated nuclei (with high level of Mef2)

257 (Figure 5). These data indicate that *zfh1-long* isoforms are transcribed in both the
258 progenitors and in muscle cells where *miR-8* regulation will prevent their translation,
259 explaining the lack of protein. In contrast, *zfh1-short* is only expressed in a few larval MPs,
260 and it is then detected at highest levels specifically in the adult pMPs. Since *zfh1-short* is
261 not susceptible to regulation by *miR-8*, its specific transcription may therefore be
262 determinant for maintaining high levels of Zfh1 in a subset of progenitors and enable them
263 to escape differentiation.

264

265 ***zfh1* isoform transcription requires Notch activity in adult SCs**

266 As expression of *zfh1-short* (*zfh1-RA*) in the adult MPs (Figure 5E) may be critical for them
267 to retain their progenitor status, there must be mechanisms that ensure this isoform is
268 appropriately transcribed. Notch is required for Zfh1 expression in MPs (Figure 3) and
269 thus may contribute to this regulation. If this is the case, expression of a constitutively
270 active Notch (Notch Δ ECD) should up regulate *zfh1-short* transcripts in the MPs at larval
271 stages when its expression is normally low. In agreement, expression of active Notch in
272 the progenitors (1151-Gal4>Notch Δ ECD) significantly increased the proportions of cells
273 transcribing *zfh1-short* (Figure 6 A-B' and C).

274 To address whether Notch is necessary for *zfh1-short* transcription in the adult pMPs, we
275 specifically depleted Notch levels after eclosion (using *Enh3-Gal4* in combination with
276 Gal80^{ts} to drive *Notch RNAi*; Figure 6 D-E'). Consistent with expression of *zfh1-short* being
277 dependent on Notch activity, the levels of *zfh1-short* were significantly reduced in the adult
278 pMPs when Notch was down-regulated after eclosion (Figure 6 D-E and G). Conversely,
279 expression of *zfh1-long* was unaffected (Figure supplement 6). Notably, Mef2 accumulated
280 to high levels in the adult pMPs under these conditions, suggesting that Notch activity
281 helps prevent their differentiation (Figure 6 D' and E'), most likely through its regulation of
282 *zfh1-short*.

283 To investigate whether *zfh1* expression in adult MPs is required to prevent them
284 differentiating, its expression was similarly downregulated in the pMPs, at 48 hours after
285 eclosion. Targeted *zfh1* down-regulation in adults resulted in high levels of Mef2 being
286 present in the adult MPs, suggesting that they had entered into the differentiation
287 programme (Figure 6F-F'). Such forced differentiation of MPs would deplete the progenitor
288 population and so should compromise muscle maintenance and repair. We therefore
289 monitored the consequences of prolonged *zfh1* depletion on adult flies, assessing their

290 phenotypes at ten days. Approximately 30% had a “held out wing” posture (n= 9/27)
291 (Figure 7A-B), a phenotype often associated with flight muscle defects (Vigoreaux, 2001).
292 The number of nuclei per muscle (DLM4) was also significantly reduced in the aged adults
293 when *zfh1* was specifically depleted in the pMPs (Figure 7D-E). As no “held out wing”
294 phenotype or muscle defects were observed in adult flies within 24 hours of knock-down,
295 the phenotypes at 10 days are due a defect in the homeostasis of the adult flight muscles,
296 consistent with *Zfh1*+ve cells contributing to their maintenance in a manner similar to the
297 mammalian satellite cells.

298

299 **DISCUSSION**

300

301 A key property of adult stem cells is their ability to remain in a quiescent state for a
302 prolonged period of time (Li and Clevers, 2010). Investigating the maintenance of
303 *Drosophila* MPs we have uncovered an important new regulatory logic, in which a switch in
304 RNA isoforms enables a sub-population of cells to escape miRNA regulation and so avoid
305 the differentiation programme. At the same time, analyzing expression of a pivotal player
306 in this regulatory loop, *zfh1*, has revealed a population of persistent progenitors associated
307 with adult muscles in *Drosophila*, that appear analogous to mammalian satellite cells
308 (Figure 7F).

309 ***Zfh1 marks a population of satellite-like cells in adult Drosophila***

310 Until now, the fly has been thought to lack a persistent muscle stem cell population,
311 leading to speculation about how its muscles could withstand the wear and tear of its
312 active lifestyle. By analyzing the expression and function of Zfh-1, we identified a
313 population of muscle-associated cells in the adult that retain progenitor-like properties,
314 marked by Zfh-1 expression. Expression in the persistent adult “satellite-like” cells is
315 dependent on one specific Zfh1 enhancer, which is directly regulated by Notch. Activity of
316 Notch is important for maintaining Zfh1 expression and hence is required to sustain the
317 progenitor status of these cells, similar to the situation in mammalian satellite cells, which
318 require Notch activity for their maintenance (Mourikis and Tajbakhsh, 2014; Bjornson, et
319 al., 2012).

320 Using lineage-tracing method we showed that adult Zfh1+ve cells, in normal conditions,
321 provide new myoblasts to the fibers. Furthermore, conditional down regulation of *zfh1* led
322 adult pMPs to enter differentiation and resulted in flight defects, evident by a held out wing
323 posture. These results demonstrate that Zfh-1 is necessary to maintain these progenitors
324 and that, similar to vertebrate satellite cells; the Zfh1+ve progenitor cells contribute to the
325 adult muscles homeostasis. Thus the retention of a pool of progenitor cells may be critical
326 to maintain the physiological function of all muscles in all organism types, as also
327 highlighted by their identification in another arthropod *Parahyle* (Alwes, et al., 2016;
328 Konstantinides and Averof, 2014). *Drosophila* notably differs because their satellite-like
329 cells do not express the Pax3/Pax7 homologue (*gooseberry*; data not shown), considered
330 a canonical marker in mammals and some other organisms (Chang and Rudnicki, 2014).
331 Instead, Zfh1 appears to fulfill an analogous function and it will be interesting to discover

332 how widespread this alternate Zfh1 pathway is for precursor maintenance. Notably, the
333 loss of ZEB1 in mice accelerates the temporal expression muscle differentiation genes (eg.
334 MHC) suggesting that there is indeed an evolutionary conserved function of Zfh1/ZEB in
335 regulating the muscle differentiation process (Siles, et al., 2013). This lends further
336 credence to the model that Zfh1 could have a fundamental role in preventing differentiation
337 that may be harnessed in multiple contexts.

338 ***Switching 3' UTR to protect progenitors from differentiation***

339 Another key feature of Zfh-1 regulation that is conserved between mammals and flies is its
340 sensitivity to the miR-200/miR-8 family of miRNAs (Antonello, et al., 2015; Brabletz and
341 Brabletz, 2010). This has major significance in many cancers, where loss of miR-200
342 results in elevated levels of ZEB1 promoting the expansion of cancer stem cells, and has
343 led to a widely accepted model in which the downregulation of Zfh1 family is necessary to
344 curb stem-ness (Brabletz and Brabletz, 2010). This fits with our observations, as we find
345 that *miR-8* is upregulated during differentiation of the MPs and suppresses Zfh1 protein
346 expression. Critically however, only some RNA isoforms, *zfh1-long*, contain seed sites
347 necessary for *miR-8* regulation (Antonello, et al., 2015). The alternate, *zfh1-short*, isoform
348 has a truncated 3'UTR that lacks the *miR-8* recognition sequences and will thus be
349 insensitive to *miR-8* regulation. Significantly, this *zfh1-short* isoform is specifically
350 expressed in MPs that persist into adulthood and hence can protect them from *miR-8*
351 induced differentiation. Furthermore, it appears that Notch activity strongly promotes *zfh1-*
352 *short* expression, explaining how this isoform is retained to sustain progenitors into adult-
353 hood.

354 Our study therefore provides a novel molecular logic explaining the maintenance of
355 *Drosophila* satellite-like cells. This relies on the expression of *zfh1-short*, which, by being
356 insensitive to *miR-8* regulation, can sustain Zfh1 protein production to protect pMPs from
357 differentiation (Figure 7F). It also implies that Notch preferentially promotes the expression
358 of a specific RNA isoform, most likely through the use of an alternate promoter in *zfh1*.
359 Both of these concepts have widespread implications.

360 Alternate use of 3'UTRs, to escape miR regulation, is potentially an important mechanism
361 to tune developmental decisions. Some tissues have a global tendency to favour certain
362 isoform types, for example, distal polyadenylation sites are preferred in neuronal tissues
363 (Zhang, et al., 2005). Furthermore, the occurrence of alternate 3'UTR RNA isoforms is
364 widespread (>50% human genes generate alternate 3'UTR isoforms) and many conserved

365 miR target sites are contained in such alternate 3'UTRs (Sandberg, et al., 2008; Tian, et
366 al., 2005). Thus, similar isoform switching may underpin many instances of progenitor
367 regulation and cell fate determination. Indeed an isoform switch appears to underlie
368 variations in Pax3 expression levels between two different populations of muscle satellite
369 cells in mice, where the use of alternative polyadenylation sites resulted in transcripts with
370 shorter 3'UTRs that are resistant to regulation by *miR-206* (Boutet, et al., 2012). The
371 selection of alternate 3'-UTRs could ensure that protein levels do not fall below a critical
372 level (Yatsenko, et al., 2014), and in this way prevent differentiation from being triggered.

373 The switch in *zfh1* RNA isoforms is associated with Notch-dependent maintenance of the
374 persistent adult MPs. Notably, *zfh1-short* is generated from an alternate promoter, as well
375 as having a truncated 3'UTR, which may be one factor underlying this switch. Studies in
376 yeasts demonstrate that looping occurs between promoters and polyadenylation sites, and
377 that specific factors recruited at promoters can influence poly-A site selection (Lamas-
378 Maceiras, et al., 2016; Tian and Manley, 2013). The levels and speed of transcription also
379 appear to influence polyA site selection (Proudfoot, 2016; Tian and Manley, 2013; Pinto, et
380 al., 2011). If Notch mediated activation via *Enh3* favors initiation at the *zfh1-short* promoter,
381 this could in turn influence the selection of the proximal adenylation site to generate the
382 truncated *miR-8* insensitive UTR. The concept that signaling can differentially regulate
383 RNA sub-types has so far been little explored but our results suggest that is potentially of
384 considerable significance. In future it will be important to investigate the extent that this
385 mechanism is deployed in other contexts where signaling coordinates cell fate choices and
386 stem cell maintenance.

387

388 **Materials and Methods**

389

390 **Drosophila Genetics.** All *Drosophila melanogaster* stocks were grown on standard
391 medium at 25°C. The following stains were used: *w*¹¹⁸ as wild type (wt), *UAS-white-RNAi*
392 as control for *RNAi* experiments (BL #35573), *UAS-zfh1-RNAi* (VDRC: KK103205 and
393 GD42856), *Mef2-Gal4* (Ranganayakulu, et al., 1996), *UAS-Mef2* (Cripps, et al., 2004),
394 *UAS-GTRACE* (BL # 28281), *UAS-Notch-RNAi* (BL #7078), *Notch[NRE]-GFP* (Simon, et
395 al., 2014), *UAS-NotchΔECD* (Chanet, et al., 2009; Fortini and Artavanis-Tsakonas, 1993;
396 Rebay, et al., 1993), *miR8-Gal4* (Karres, et al., 2007), *UAS-miR8* (Vallejo, et al., 2011),
397 *UAS-mCD8::GFP* (BL # 5137), *UAS-GFPnls* (BL # 65402), *UAS-Src::GFP* (Kaltschmidt, et
398 al., 2000), *MHC-lacZ* (Hess et al., 1989), *1151-Gal4* (Anant, et al., 1998), *miR-8-sensor-*
399 *EGFP* (Kennell, et al., 2012). *RNAi* experiments were conducted at 29°C and *TubGal80^{ts}*
400 (McGuire, et al., 2003) was used to limit *RNAi* expression to a defined period of time.
401 Enhancer-Gal4 lines described in Figure 2 and Figure supplement S3 are either from
402 Janelia FlyLight (<http://flweb.janelia.org>) or Vienna Tiles Library
403 (<http://stockcenter.vdrc.at/control/main>).

404

405 **Immunohistochemistry and *in situ* hybridization.** Immunofluorescence stainings of
406 wing discs were performed using standard techniques. Adult muscles were prepared and
407 stained as described (Hunt and Demontis, 2013). The following primary antibody were
408 used: Rabbit anti-Zfh1 (1:5000, a gift from Ruth Lehmann, New York, USA), Mouse anti-
409 Cut (1:20, DSHB), Rabbit anti-β3-Tubulin (1:5000, a gift from Renate Renkawitz-Pohl,
410 Marburg, Germany), Rat anti-Tropomyosin (1:1000, Abcam, ab50567), Goat anti-GFP
411 (1:200, Abcam, ab6673), Rabbit anti-Ds-Red (1:25; Clontech, 6324496), Rabbit anti-Mef2
412 (1:200, a gift from Eileen Furlong, Heidelberg, Germany), Mouse anti-P1 (1:20, a gift from
413 István Andó, Szeged, Hungary), Mouse anti-PH3 (1:100, Cell Signaling Technology, #9706),
414 Mouse anti-β-Gal (1:1000, Promega, Z378A), Alexa-conjugated Phalloidin (1:200, Thermo
415 fisher), Rat anti-Dcad2 (1:200, DSHB). *In situ* experiments were carried out according to
416 Stellaris-protocols
417 (https://www.biosearchtech.com/assets/bti_custom_stellaris_drosophila_protocol.pdf).
418 Antibodies were included to the overnight hybridization step (together with the probes).
419 *zfh1* probes were generated by BioResearch Technologies. The sequence used for *zfh1-*

420 *short* probe span 393bp of the first *zfh1*-RA exon, for *zfh1-long* probe, the sequence of the
421 third exon (711bp) common to both *zfh1*-RB and *zfh1*-RE was used (see Figure 5).

422 **Construction of reporter lines and mutagenesis.** For Enh3-GFP reporter line, the
423 genomic region chr3R : 30774595..30778415 (Enh3/GMR35H09) according to Flybase
424 genome release r6.03 was amplified using *yw* genomic DNA as template. Enh3 fragment
425 was then cloned into the pGreenRabbit vector (Housden, et al., 2012). For *Enh3[mut]-GFP*
426 line, two Su(H) binding sites were predicted within Enh3 sequence using Patser (Hertz and
427 Stormo, 1999) and mutated by PCR based approach with primers overlapping the Su(H)
428 sites to be mutated with the following sequence modifications : Su(H)1 AGTGGGAA to
429 AGGTGTGA and Su(H) 2 TTCTCACA to TGTTTGCA. Both constructs were inserted at
430 position 68A4 on the third chromosome by injection into *nos-phiC31-NLS; attP2* embryos
431 (Bischof, et al., 2007).

432 **CRISPR/Cas9 genome editing.** CRISPR mediated deletion of Enh3 was performed
433 according to (Port, et al., 2014) For generating guide RNAs, two protospacers were
434 selected (sgRNA1 GCATTCCGCAGGTTTAGTCAC and sgRNA2
435 GCGATAACCCGGCGACCTCC) flanking 5' and 3' Enhancer-3 regions,
436 (<http://www.flyrnai.org/crispr/>). The protospacers were cloned into the tandem guide RNA
437 expression vector pCFD4 (Addgene # 49411) ([http://www.crisprflydesign.org/wp-](http://www.crisprflydesign.org/wp-content/uploads/2014/06/Cloning-with-pCFD4.pdf)
438 [content/uploads/2014/06/Cloning-with-pCFD4.pdf](http://www.crisprflydesign.org/wp-content/uploads/2014/06/Cloning-with-pCFD4.pdf)). For the homology directed repair step,
439 two homology arms were amplified using *yw* genomic DNA as template with the following
440 primers (Homology arm1: Fwd. 5' GCGCGAATTCGGGCTAAACGCCAGATAAGCG 3'
441 Rev. 5' TTCCGCGGCCGCC ACTGGATTCCACGGCTTTTCG 3'– Homology arm 2: Fwd.
442 5' GGTAGCTCTTCTTA TATAACCCGGCGACCTCCTCG 3' Rev. 5'
443 GGTAGCTCTTCTGACCGGAC GAAAACTAGCGACC) and cloned into the pDsRed-attP
444 (Addgene # 51019) vector (<http://flycrispr.molbio.wisc.edu/protocols/pHD-DsRed-attP>).
445 Both constructs were injected into *nos-Cas9* (BL # 54591) embryos. Flies mutant for
446 Enhancer 3 were screened for the expression of the Ds-Red in the eyes and confirmed
447 with sequencing of PCR fragment spanning the deletion.

448 **Microscopy and data analysis.** Samples were imaged on Leica SP2 or TCS SP8
449 microscopes (CAIC, University of Cambridge) at 20X or 40X magnification and 1024/1024
450 pixel resolution. Images were processed with Image J and assembled with Adobe
451 Illustrator. Quantification of fluorescence signal intensities was performed with Image J
452 software. In each case the n refers to the number of individual specimens analyzed, which
453 were from two or more independent experiments. For experiments to compare and

454 measure expression levels, samples were prepared and analyzed in parallel, with identical
455 conditions and the same laser parameters used for image acquisition. For each confocal
456 stack a Sum slices projections was generated. Signal intensities were obtained by
457 manually outlining the regions of interest, based on expression of markers, and measuring
458 the average within each region. The values were then normalized to similar background
459 measurements for each sample. In Figure 6 the number of transcriptional *zfh1-short* dots
460 was counted manually with Image J and normalized to the total number of nuclei (Zfh1
461 staining), which was determined by a Matlab homemade script. Graphs and statistical
462 analysis were performed with Prism 7 using unpaired t-test. Error bars indicate standard
463 error of the mean.

464 **Quantitative RT PCR.** 30 Wing Imaginal discs from each genotype were dissected and
465 RNA isolated using TRIzol (Life technologies). Quantitative PCR were performed as
466 described (Krejci and Bray, 2007). Values were normalized to the level of *Rpl32*. The
467 following primers were used. *Rpl32*, Fwd 5'-ATGCTAAGCTGTCGCACAAATG-3' and Rev
468 5'-GTTTCGATCCGTAACCGATGT-3'. *zfh1* Fwd 5'- GTTCAAGCACCACTCAAGGAG-3'
469 and Rev 5'- CTTCTTGGAGGTCATGTGGGAGG-3'. (Product common to all three
470 *zfh1* isoforms).

471 **Acknowledgements**

472
473 We thank the Bloomington Stock Center, the VDRC Stock Center and the Developmental
474 Studies Hybridoma Bank for *Drosophila* strains and antibodies. We acknowledge Ruth
475 Lehmann, Renate Renkawitz-Pohl, Eileen Furlong and István Andó for antibodies. We
476 thank Eva Zacharioudaki, Alain Vincent and Michalis Averof for critical reading of the
477 manuscript and other members of SJB lab for valuable discussion. This work was funded
478 by a programme grant from the MRC to SJB and by an EMBO Long Term Fellowship for
479 HB.

480

481 **Competing interest**

482 The authors declare that they have no competing interests.

483

484 **REFERENCES**

485 Alwes, F., Enjolras, C., and Averof, M. (2016). Live imaging reveals the progenitors and
486 cell dynamics of limb regeneration. *Elife* 5.10.7554/eLife.19766

- 487 Anant, S., Roy, S., and VijayRaghavan, K. (1998). Twist and Notch negatively regulate
488 adult muscle differentiation in *Drosophila*. *Development* 125, 1361-9
- 489 Antonello, Z.A., Reiff, T., Ballesta-Illan, E., and Dominguez, M. (2015). Robust intestinal
490 homeostasis relies on cellular plasticity in enteroblasts mediated by miR-8-Escargot switch.
491 *EMBO J* 34, 2025-41.10.15252/embj.201591517
- 492 Aradhya, R., Zmojdzian, M., Da Ponte, J.P., and Jagla, K. (2015). Muscle niche-driven
493 Insulin-Notch-Myc cascade reactivates dormant Adult Muscle Precursors in *Drosophila*.
494 *Elife* 4.10.7554/eLife.08497
- 495 Benlhabib, H., Guo, W., Pierce, B.M., and Mendelson, C.R. (2015). The miR-200 family
496 and its targets regulate type II cell differentiation in human fetal lung. *J Biol Chem* 290,
497 22409-22.10.1074/jbc.M114.636068
- 498 Bernard, F., Dutriaux, A., Silber, J., and Lalouette, A. (2006). Notch pathway repression by
499 vestigial is required to promote indirect flight muscle differentiation in *Drosophila*
500 *melanogaster*. *Dev Biol* 295, 164-77.10.1016/j.ydbio.2006.03.022
- 501 Bernard, F., Krejci, A., Housden, B., Adryan, B., and Bray, S.J. (2010). Specificity of Notch
502 pathway activation: twist controls the transcriptional output in adult muscle progenitors.
503 *Development* 137, 2633-42.10.1242/dev.053181
- 504 Bischof, J., Maeda, R.K., Hediger, M., Karch, F., and Basler, K. (2007). An optimized
505 transgenesis system for *Drosophila* using germ-line-specific phiC31 integrases. *Proc Natl*
506 *Acad Sci U S A* 104, 3312-7.10.1073/pnas.0611511104
- 507 Bjornson, C.R., Cheung, T.H., Liu, L., Tripathi, P.V., Steeper, K.M., and Rando, T.A.
508 (2012). Notch signaling is necessary to maintain quiescence in adult muscle stem cells.
509 *Stem Cells* 30, 232-42.10.1002/stem.773
- 510 Boutet, S.C., Cheung, T.H., Quach, N.L., Liu, L., Prescott, S.L., Edalati, A., Iori, K., and
511 Rando, T.A. (2012). Alternative polyadenylation mediates microRNA regulation of muscle
512 stem cell function. *Cell Stem Cell* 10, 327-36.10.1016/j.stem.2012.01.017
- 513 Brabletz, S., and Brabletz, T. (2010). The ZEB/miR-200 feedback loop--a motor of cellular
514 plasticity in development and cancer? *EMBO Rep* 11, 670-7.10.1038/embor.2010.117
- 515 Chanet, S., Vodovar, N., Mayau, V., and Schweisguth, F. (2009). Genome engineering-
516 based analysis of Bearded family genes reveals both functional redundancy and a
517 nonessential function in lateral inhibition in *Drosophila*. *Genetics* 182, 1101-
518 8.10.1534/genetics.109.105023
- 519 Chang, N.C., and Rudnicki, M.A. (2014). Satellite cells: the architects of skeletal muscle.
520 *Curr Top Dev Biol* 107, 161-81.10.1016/B978-0-12-416022-4.00006-8

- 521 Chaturvedi, D., Reichert, H., and VijayRaghavan, K. (2017). Identification and Functional
522 Characterization of Muscle Satellite Cells in *Drosophila*. bioRxiv
523 <http://dx.doi.org/10.1101/037838>
- 524 Cripps, R.M., Lovato, T.L., and Olson, E.N. (2004). Positive autoregulation of the Myocyte
525 enhancer factor-2 myogenic control gene during somatic muscle development in
526 *Drosophila*. *Dev Biol* 267, 536-47.10.1016/j.ydbio.2003.12.004
- 527 Elgar, S.J., Han, J., and Taylor, M.V. (2008). *mef2* activity levels differentially affect gene
528 expression during *Drosophila* muscle development. *Proc Natl Acad Sci U S A* 105, 918-
529 23.10.1073/pnas.0711255105
- 530 Evans, C.J., Olson, J.M., Ngo, K.T., Kim, E., Lee, N.E., Kuoy, E., Patananan, A.N., Sitz, D.,
531 Tran, P., Do, M.T., et al. (2009). G-TRACE: rapid Gal4-based cell lineage analysis in
532 *Drosophila*. *Nat Methods* 6, 603-U70.10.1038/nmeth.1356
- 533 Figeac, N., Daczewska, M., Marcelle, C., and Jagla, K. (2007). Muscle stem cells and
534 model systems for their investigation. *Dev Dyn* 236, 3332-42.10.1002/dvdy.21345
- 535 Figeac, N., Jagla, T., Aradhya, R., Da Ponte, J.P., and Jagla, K. (2010). *Drosophila* adult
536 muscle precursors form a network of interconnected cells and are specified by the
537 rhomboid-triggered EGF pathway. *Development* 137, 1965-73.10.1242/dev.049080
- 538 Fortini, M.E., and Artavanis-Tsakonas, S. (1993). Notch: neurogenesis is only part of the
539 picture. *Cell* 75, 1245-7
- 540 Gunage, R.D., Reichert, H., and VijayRaghavan, K. (2014). Identification of a new stem
541 cell population that generates *Drosophila* flight muscles. *Elife* 3.10.7554/eLife.03126
- 542 Hertz, G.Z., and Stormo, G.D. (1999). Identifying DNA and protein patterns with
543 statistically significant alignments of multiple sequences. *Bioinformatics* 15, 563-77
- 544 Housden, B.E., Millen, K., and Bray, S.J. (2012). *Drosophila* Reporter Vectors Compatible
545 with PhiC31 Integrase Transgenesis Techniques and Their Use to Generate New Notch
546 Reporter Fly Lines. *G3 (Bethesda)* 2, 79-82.10.1534/g3.111.001321
- 547 Hunt, L.C., and Demontis, F. (2013). Whole-mount immunostaining of *Drosophila* skeletal
548 muscle. *Nat Protoc* 8, 2496-501.10.1038/nprot.2013.156
- 549 Jenett, A., Rubin, G.M., Ngo, T.T., Shepherd, D., Murphy, C., Dionne, H., Pfeiffer, B.D.,
550 Cavallaro, A., Hall, D., Jeter, J., et al. (2012). A GAL4-driver line resource for *Drosophila*
551 neurobiology. *Cell Rep* 2, 991-1001.10.1016/j.celrep.2012.09.011
- 552 Jory, A., Estella, C., Giorgianni, M.W., Slattery, M., Lavery, T.R., Rubin, G.M., and Mann,
553 R.S. (2012). A survey of 6,300 genomic fragments for cis-regulatory activity in the imaginal
554 discs of *Drosophila melanogaster*. *Cell Rep* 2, 1014-24.10.1016/j.celrep.2012.09.010

- 555 Kaltschmidt, J.A., Davidson, C.M., Brown, N.H., and Brand, A.H. (2000). Rotation and
556 asymmetry of the mitotic spindle direct asymmetric cell division in the developing central
557 nervous system. *Nat Cell Biol* 2, 7-12.10.1038/71323
- 558 Karres, J.S., Hilgers, V., Carrera, I., Treisman, J., and Cohen, S.M. (2007). The conserved
559 microRNA miR-8 tunes atrophin levels to prevent neurodegeneration in *Drosophila*. *Cell*
560 131, 136-45.10.1016/j.cell.2007.09.020
- 561 Kennell, J.A., Cadigan, K.M., Shakhmantsir, I., and Waldron, E.J. (2012). The microRNA
562 miR-8 is a positive regulator of pigmentation and eclosion in *Drosophila*. *Dev Dyn* 241,
563 161-8.10.1002/dvdy.23705
- 564 Konstantinides, N., and Averof, M. (2014). A common cellular basis for muscle
565 regeneration in arthropods and vertebrates. *Science* 343, 788-
566 91.10.1126/science.1243529
- 567 Korpai, M., Lee, E.S., Hu, G., and Kang, Y. (2008). The miR-200 family inhibits epithelial-
568 mesenchymal transition and cancer cell migration by direct targeting of E-cadherin
569 transcriptional repressors ZEB1 and ZEB2. *J Biol Chem* 283, 14910-
570 4.10.1074/jbc.C800074200
- 571 Krejci, A., Bernard, F., Housden, B.E., Collins, S., and Bray, S.J. (2009). Direct response
572 to Notch activation: signaling crosstalk and incoherent logic. *Sci Signal* 2,
573 ra1.10.1126/scisignal.2000140
- 574 Krejci, A., and Bray, S. (2007). Notch activation stimulates transient and selective binding
575 of Su(H)/CSL to target enhancers. *Genes Dev* 21, 1322-7.10.1101/gad.424607
- 576 Lamas-Maceiras, M., Singh, B.N., Hampsey, M., and Freire-Picos, M.A. (2016). Promoter-
577 Terminator Gene Loops Affect Alternative 3'-End Processing in Yeast. *J Biol Chem* 291,
578 8960-8.10.1074/jbc.M115.687491
- 579 Li, L., and Clevers, H. (2010). Coexistence of quiescent and active adult stem cells in
580 mammals. *Science* 327, 542-5.10.1126/science.1180794
- 581 Manning, L., Heckscher, E.S., Purice, M.D., Roberts, J., Bennett, A.L., Kroll, J.R., Pollard,
582 J.L., Strader, M.E., Lupton, J.R., Dyukareva, A.V., et al. (2012). A resource for
583 manipulating gene expression and analyzing cis-regulatory modules in the *Drosophila*
584 CNS. *Cell Rep* 2, 1002-13.10.1016/j.celrep.2012.09.009
- 585 McGuire, S.E., Le, P.T., Osborn, A.J., Matsumoto, K., and Davis, R.L. (2003).
586 Spatiotemporal rescue of memory dysfunction in *Drosophila*. *Science* 302, 1765-
587 8.10.1126/science.1089035

- 588 Mourikis, P., Gopalakrishnan, S., Sambasivan, R., and Tajbakhsh, S. (2012). Cell-
589 autonomous Notch activity maintains the temporal specification potential of skeletal
590 muscle stem cells. *Development* 139, 4536-48.10.1242/dev.084756
- 591 Mourikis, P., and Tajbakhsh, S. (2014). Distinct contextual roles for Notch signalling in
592 skeletal muscle stem cells. *BMC Dev Biol* 14, 2.10.1186/1471-213X-14-2
- 593 Park, S.M., Gaur, A.B., Lengyel, E., and Peter, M.E. (2008). The miR-200 family
594 determines the epithelial phenotype of cancer cells by targeting the E-cadherin repressors
595 ZEB1 and ZEB2. *Genes Dev* 22, 894-907.10.1101/gad.1640608
- 596 Pinto, P.A., Henriques, T., Freitas, M.O., Martins, T., Domingues, R.G., Wyrzykowska,
597 P.S., Coelho, P.A., Carmo, A.M., Sunkel, C.E., Proudfoot, N.J., et al. (2011). RNA
598 polymerase II kinetics in polo polyadenylation signal selection. *EMBO J* 30, 2431-
599 44.10.1038/emboj.2011.156
- 600 Port, F., Chen, H.M., Lee, T., and Bullock, S.L. (2014). Optimized CRISPR/Cas tools for
601 efficient germline and somatic genome engineering in *Drosophila*. *Proc Natl Acad Sci U S*
602 *A* 111, E2967-76.10.1073/pnas.1405500111
- 603 Postigo, A.A., and Dean, D.C. (1999). ZEB represses transcription through interaction with
604 the corepressor CtBP. *Proc Natl Acad Sci U S A* 96, 6683-8
- 605 Postigo, A.A., Ward, E., Skeath, J.B., and Dean, D.C. (1999). *zfh-1*, the *Drosophila*
606 homologue of ZEB, is a transcriptional repressor that regulates somatic myogenesis. *Mol*
607 *Cell Biol* 19, 7255-63
- 608 Proudfoot, N.J. (2016). Transcriptional termination in mammals: Stopping the RNA
609 polymerase II juggernaut. *Science* 352, aad9926.10.1126/science.aad9926
- 610 Ranganayakulu, G., Schulz, R.A., and Olson, E.N. (1996). Wingless signaling induces
611 nautilus expression in the ventral mesoderm of the *Drosophila* embryo. *Dev Biol* 176, 143-
612 8.10.1006/dbio.1996.9987
- 613 Rebay, I., Fehon, R.G., and Artavanis-Tsakonas, S. (1993). Specific truncations of
614 *Drosophila* Notch define dominant activated and dominant negative forms of the receptor.
615 *Cell* 74, 319-29
- 616 Sandberg, R., Neilson, J.R., Sarma, A., Sharp, P.A., and Burge, C.B. (2008). Proliferating
617 cells express mRNAs with shortened 3' untranslated regions and fewer microRNA target
618 sites. *Science* 320, 1643-7.10.1126/science.1155390
- 619 Siles, L., Sanchez-Tillo, E., Lim, J.W., Darling, D.S., Kroll, K.L., and Postigo, A. (2013).
620 ZEB1 imposes a temporary stage-dependent inhibition of muscle gene expression and
621 differentiation via CtBP-mediated transcriptional repression. *Mol Cell Biol* 33, 1368-
622 82.10.1128/MCB.01259-12

- 623 Simon, R., Aparicio, R., Housden, B.E., Bray, S., and Busturia, A. (2014). *Drosophila* p53
624 controls Notch expression and balances apoptosis and proliferation. *Apoptosis* 19, 1430-
625 43.10.1007/s10495-014-1000-5
- 626 Sudarsan, V., Anant, S., Guptan, P., VijayRaghavan, K., and Skaer, H. (2001). Myoblast
627 diversification and ectodermal signaling in *Drosophila*. *Dev Cell* 1, 829-39
- 628 Tian, B., Hu, J., Zhang, H., and Lutz, C.S. (2005). A large-scale analysis of mRNA
629 polyadenylation of human and mouse genes. *Nucleic Acids Res* 33, 201-
630 12.10.1093/nar/gki158
- 631 Tian, B., and Manley, J.L. (2013). Alternative cleavage and polyadenylation: the long and
632 short of it. *Trends Biochem Sci* 38, 312-20.10.1016/j.tibs.2013.03.005
- 633 Vallejo, D.M., Caparros, E., and Dominguez, M. (2011). Targeting Notch signalling by the
634 conserved miR-8/200 microRNA family in development and cancer cells. *EMBO J* 30, 756-
635 69.10.1038/emboj.2010.358
- 636 Vandewalle, C., Van Roy, F., and Berx, G. (2009). The role of the ZEB family of
637 transcription factors in development and disease. *Cell Mol Life Sci* 66, 773-
638 87.10.1007/s00018-008-8465-8
- 639 Vigoreaux, J.O. (2001). Genetics of the *Drosophila* flight muscle myofibril: a window into
640 the biology of complex systems. *Bioessays* 23, 1047-63.10.1002/bies.1150
- 641 Yatsenko, A.S., Marrone, A.K., and Shcherbata, H.R. (2014). miRNA-based buffering of
642 the cobblestone-lissencephaly-associated extracellular matrix receptor dystroglycan via its
643 alternative 3'-UTR. *Nat Commun* 5, 4906.10.1038/ncomms5906
- 644 Zaravinos, A. (2015). The Regulatory Role of MicroRNAs in EMT and Cancer. *J Oncol*
645 2015, 865816.10.1155/2015/865816
- 646 Zhang, H., Lee, J.Y., and Tian, B. (2005). Biased alternative polyadenylation in human
647 tissues. *Genome Biol* 6, R100.10.1186/gb-2005-6-12-r100

648

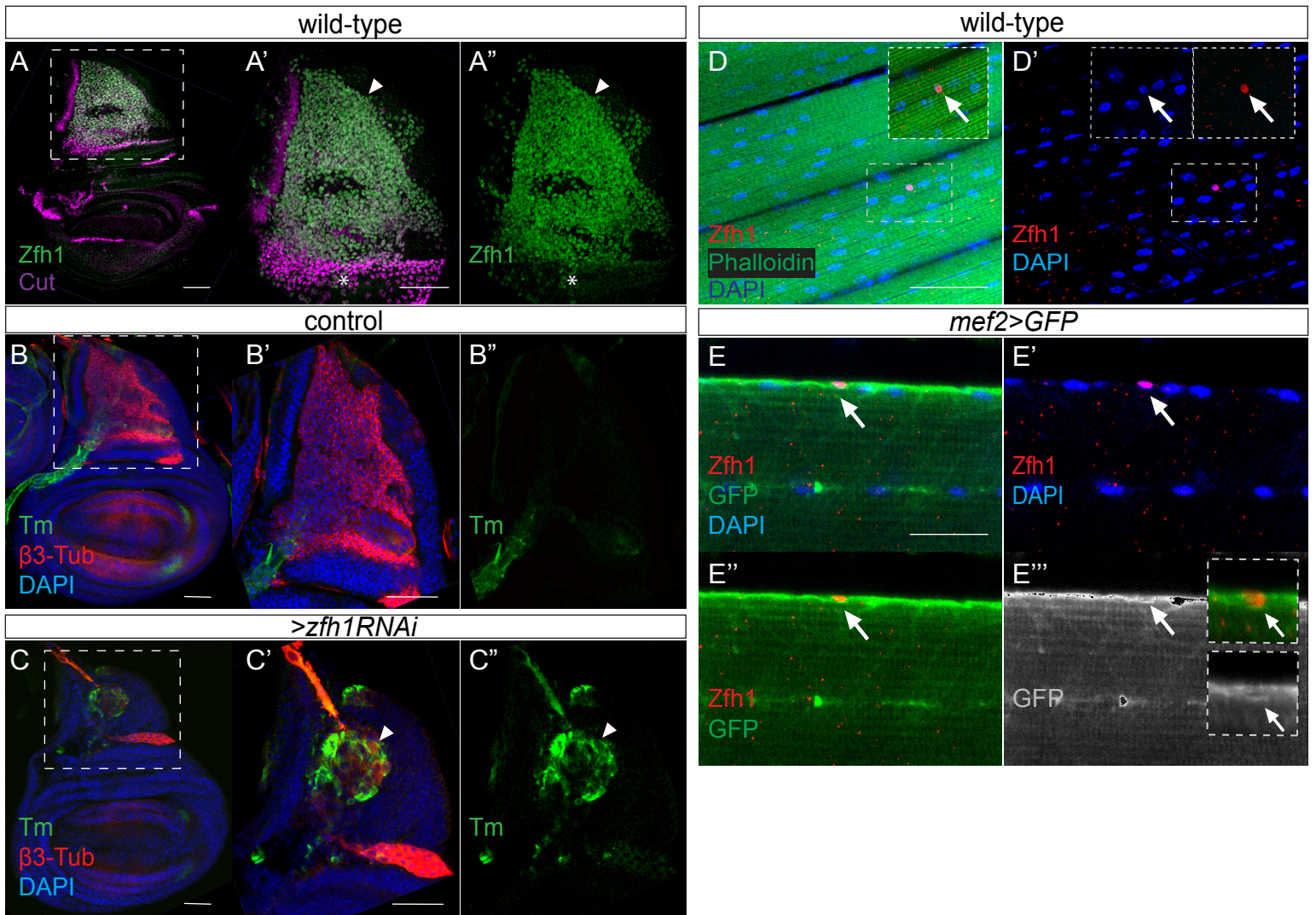


Figure 1. Zfh1 expression and function in MPs and in adult pMPs.

(A-A''). Zfh1 (Green) and Cut (Purple) expression in MPs associated with third instar wing discs, **(A'-A'')**. higher magnification (3X) of boxed region in A. Zfh1 is present in all MPs, but those with highest Cut expression have lower levels of Zfh1 (asterisk). Scale bars: 50 μ M. **(B-C)**. Down regulation of *zfh1* in MPs induces premature differentiation of the MPs (arrowhead in C'-C''). β 3-Tubulin (β 3-Tub, red) and Tropomyosin (Tm, Green) expression in control (B, *1151-Gal4>UAS-wRNAi*) and Zfh1 depleted (C, *1151-Gal4>UAS-Zfh1RNAi*) third instar wing discs, **(B'-C'')** higher magnification (3X) of boxed regions in B and C. **(D-D')**. Zfh1 expression (red) indicates the existence of persistent muscle progenitors (pMPs; arrows) associated with the muscle fibers (Phalloidin (Green), DNA/Nuclei (Blue)). The immune cell marker P1 was included in the immunostaining and is absent from the pMPs (Figure supplement 1). Scale bars: 50 μ M. **(E-E'')**. Zfh1 (Red) expressing pMPs (e.g. arrows in E'') are closely embedded in the muscle lamina of the adult indirect flight muscles and express Mef2 (myogenic cells; *Mef2-Gal4>UAS-Src::GFP*, green). Nuclei (Blue), Scale bars: 25 μ M.

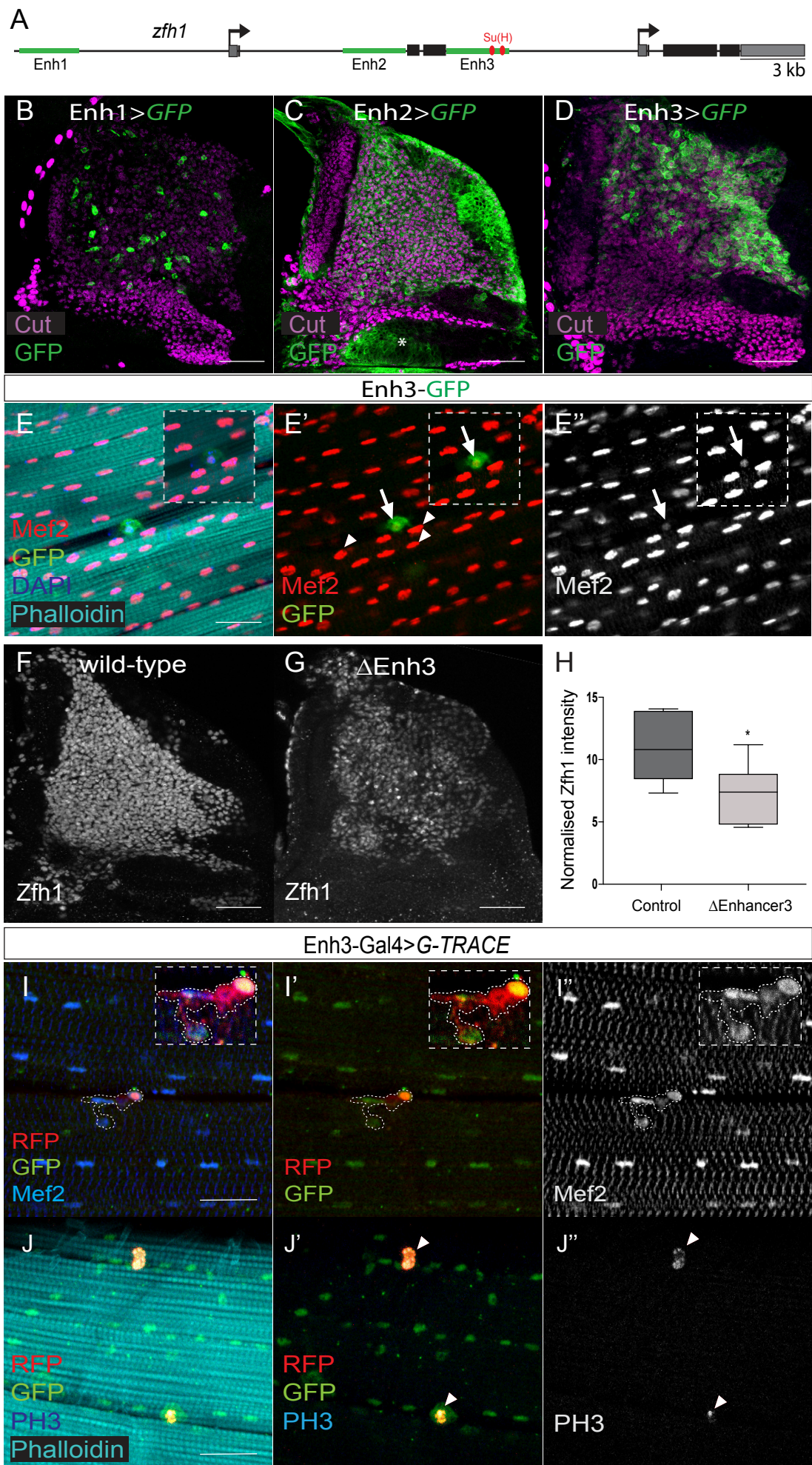


Figure 2. Regulation of *zfh1* in MPs and adult pMPs.

Figure 2. Regulation of *zfh1* in MPs and adult pMPs. (A). Schematic view of *zfh1* genomic region, *zfh1* regulatory enhancers are represented by green rectangles and arrows indicate transcription starts. Coding exons and untranslated regions are represented in black and grey boxes, respectively. **(B-D).** Three different *zfh1* enhancers are active in the MPs (labelled with Cut, purple). *Enh1-Gal4* (VT050105, B) drives GFP (Green) in a subset of scattered MPs; *Enh2-Gal4* (VT050115, C) drives GFP throughout the MPs, and in some non-MP cells (Asterisk); *Enh3-Gal4* (GMR35H09, D) is highly expressed in a subset of MPs located in the posterior region of the notum. Scale bars: 50 μ M. **(E-E'').** *Enh3-GFP* (Green) expression is retained in pMPs (characterised by low level of Mef2, red; arrows E'-E'') but not in differentiated muscle nuclei (high Mef2, red; arrowheads E'-E''). Phalloidin marks muscles and DAPI labels all nuclei (Blue). Insets: boxed regions magnified 12.5 X. Scale bars : 25 μ M. **(F-H).** *Zfh1* (white) expression in MPs is significantly reduced in discs from *Enh3* deletion Δ *Enh3* (G, H) compared to controls (F, H). (* $p= 0.0379$, $n =13$, Student t-test). Scale bars: 50 μ M. **(I-J'').** Lineage tracing shows that adult pMPs contribute to muscles. Indirect flight muscles from adult flies where *Enh3-Gal4* drives expression of the G-Trace cassette; GFP (Green) indicates myoblasts that have expressed *Enh3-Gal4*, RFP (red) indicates myoblasts where Gal4 is still active, Mef2 labels muscle nuclei (Blue). Insets: boxed regions magnified 20 X. **(J-J'').** pMPs are mitotically active, indicated by anti-phosphH3 (Blue, arrowheads J'-J'').

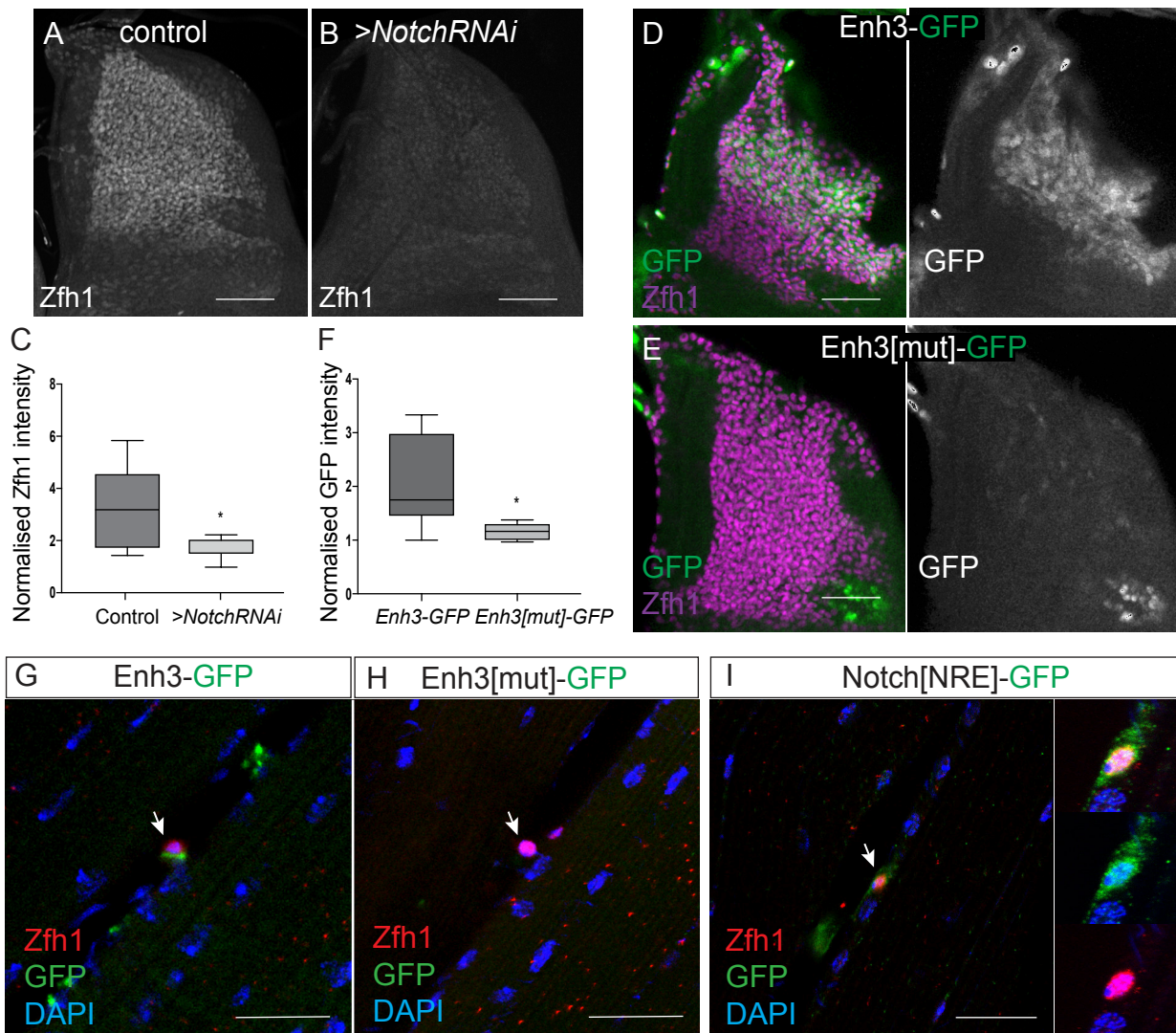


Figure 3. Notch directs Zfh1 expression in MPs and pMPs.

(A-C). Zfh1 level (white) is significantly reduced when *Notch* is down regulated. Expression of Zfh1 in MPs (A) is severely reduced in the presence of *Notch RNAi* (B, *1151-Gal4>UAS-NotchRNAi*), Scale Bars: 50 μ M. (C) Quantification of Zfh1 expression levels (* $p < 0.05$, $n = 12$). **(D-F).** Enh3 (D, *Enh3-GFP*, green) expression in MPs (purple, Zfh1) is abolished when Su(H) motifs are mutated (E, *Enh3[mut]-GFP*). Scale bars: 50 μ M. (F) Intensity of expression from *Enh3* and *Enh3[mut]* was significantly different (* $p = 0.022$, $n = 14$, Student t-test). **(G-H).** Enh3 (G, *Enh3-GFP*, green) expression in adult pMPs (red, Zfh1) is abolished when Su(H) motifs are mutated (H, *Enh3[mut]-GFP*, green), DAPI (blue) reveals all nuclei. **(I).** *Notch[NRE]-GFP* (green) is co-expressed with Zfh1 (red) in the pMPs associated with the indirect flight muscle; DAPI (Blue) detects all nuclei. (N=12 pMPs). In G-I anti-P1 was included to label immune cells and exclude them from the analysis. Scale bars: 25 μ M.

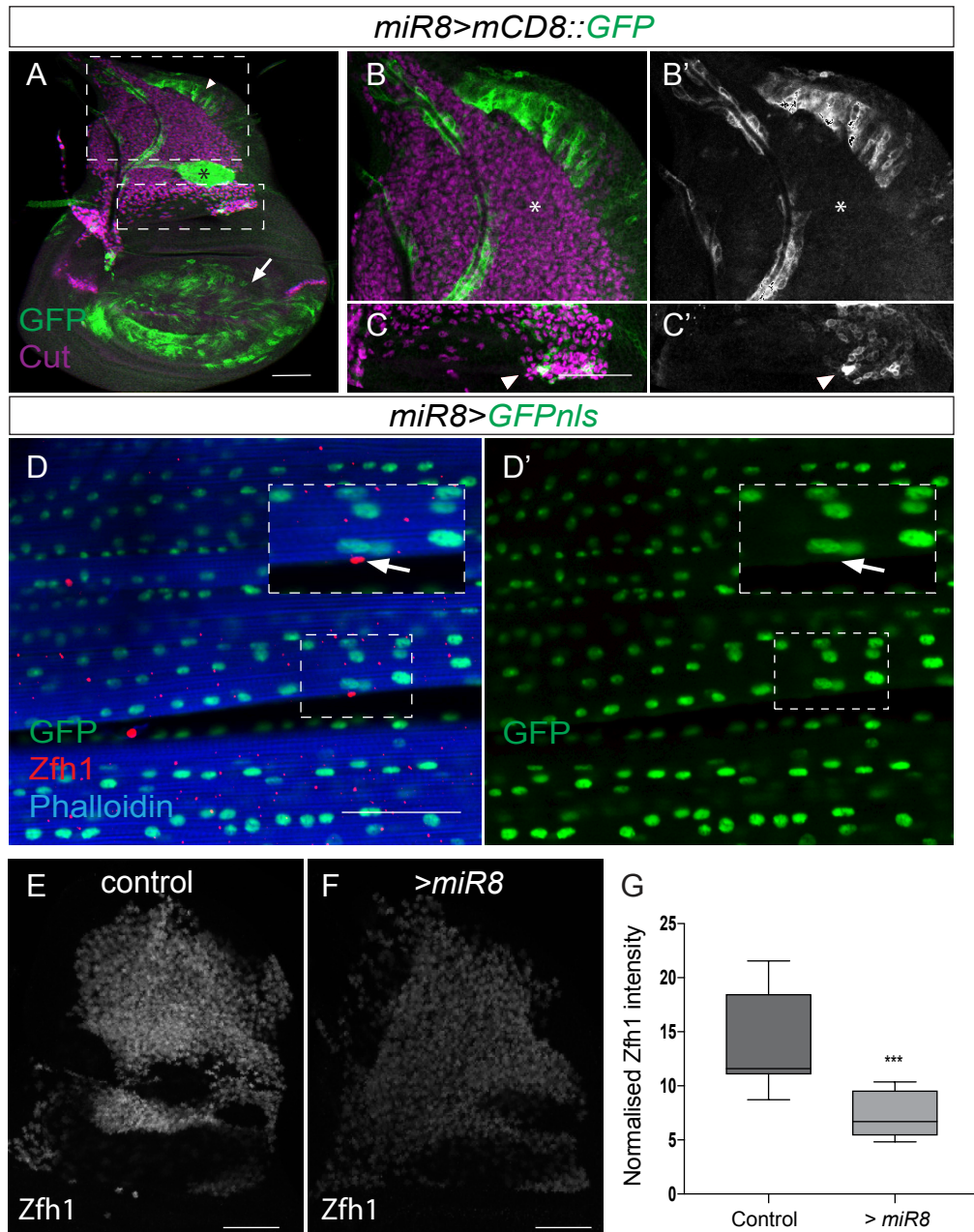


Figure 4. The conserved MicroRNA *miR-8/miR-200* antagonizes *zfh1* to promote muscle differentiation.

(A-C). Expression of *miR-8* is complementary to *Zfh1*; *miR-8* (green, *miR-8-Gal4>UAS-mCD8::GFP*) is not highly expressed in MPs (*Cut*, Purple) but is prevalent in the wing disc pouch (arrow), notum (arrowhead) and air sac (asterisk). Higher magnification shows that some *miR-8* expression can be detected in MPs where *Zfh1* is normally low (arrowhead in C) but not in other MPs. Scale bars: 50 μ M. **(D-D')** *miR-8* (green; *miR-8-Gal4>UAS-nlsGFP*) expression is absent from *Zfh1*+ve (red) pMPs (arrows, D-D') but is present at uniformly high levels in IFMs, (phalloidin, blue). Scale bars: 50 μ M. **(E-G).** Effect of *miR-8* overexpression (*1151-Gal4>UAS-miR-8*) on *Zfh1* (white) protein level in MPs. Scale Bars: 50 μ M. **(G)** *Zfh1* expression is significantly reduced by *miR-8* over-expression. (***) $p = 0.0009$, $n = 11$, Student t-test).

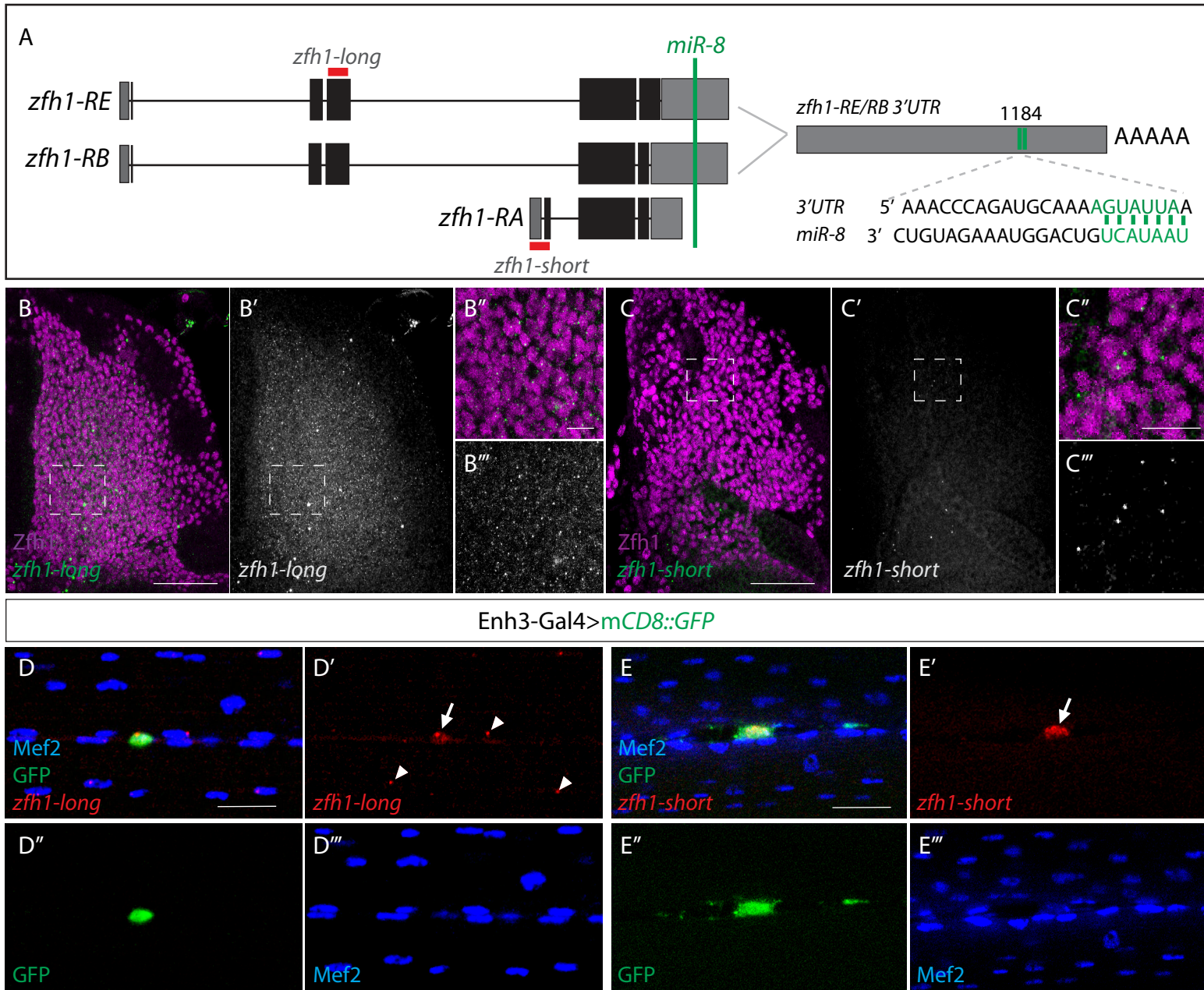


Figure 5. *zfh1* escapes *mir-8* regulation via a variable 3'UTR.

A. Schematic representation of *zfh1* isoforms. *zfh1-short* (*zfh1-RA*) is initiated from a different transcription start site and has shorter 3'UTR that lack the target site for *mir-8* (green;(Antonello, et al., 2015)) present in *zfh1-long* isoforms (*zfh1-RB*, *zfh1-RE*); the position of the *mir-8* seed sites in *zfh1-long* 3' UTR are depicted. Non-coding exons and coding exons are depicted by grey and black boxes respectively, red lines indicate the probes used for FISH experiments in B-E. **(B-C).** *zfh1-long* is present uniformly in MPs (B, green; B', white) whereas *zfh1-short* is only detected in a few MPs (C, green; C', white), detected by *in situ hybridisation* in wild type third instar wing discs stained for *Zfh1* (Purple). Scale bars: 10 μ M. (B'',B''',C''C''') Higher magnifications of boxed regions (Scale bars : 50 μ M). **(D-E).** In adult IFMs *zfh1-long* is detected in the pMPs (arrow in D') and in some differentiated nuclei located in their vicinity (arrowheads in D') whereas *zfh1-short* is only present in pMPs (arrow in E'). *Enh3* expression (green, *Enh3-Gal4>UAS-mCD8GFP*) labels adult pMPs and *Mef2* labels all muscle nuclei. Scale bars: 20 μ M.

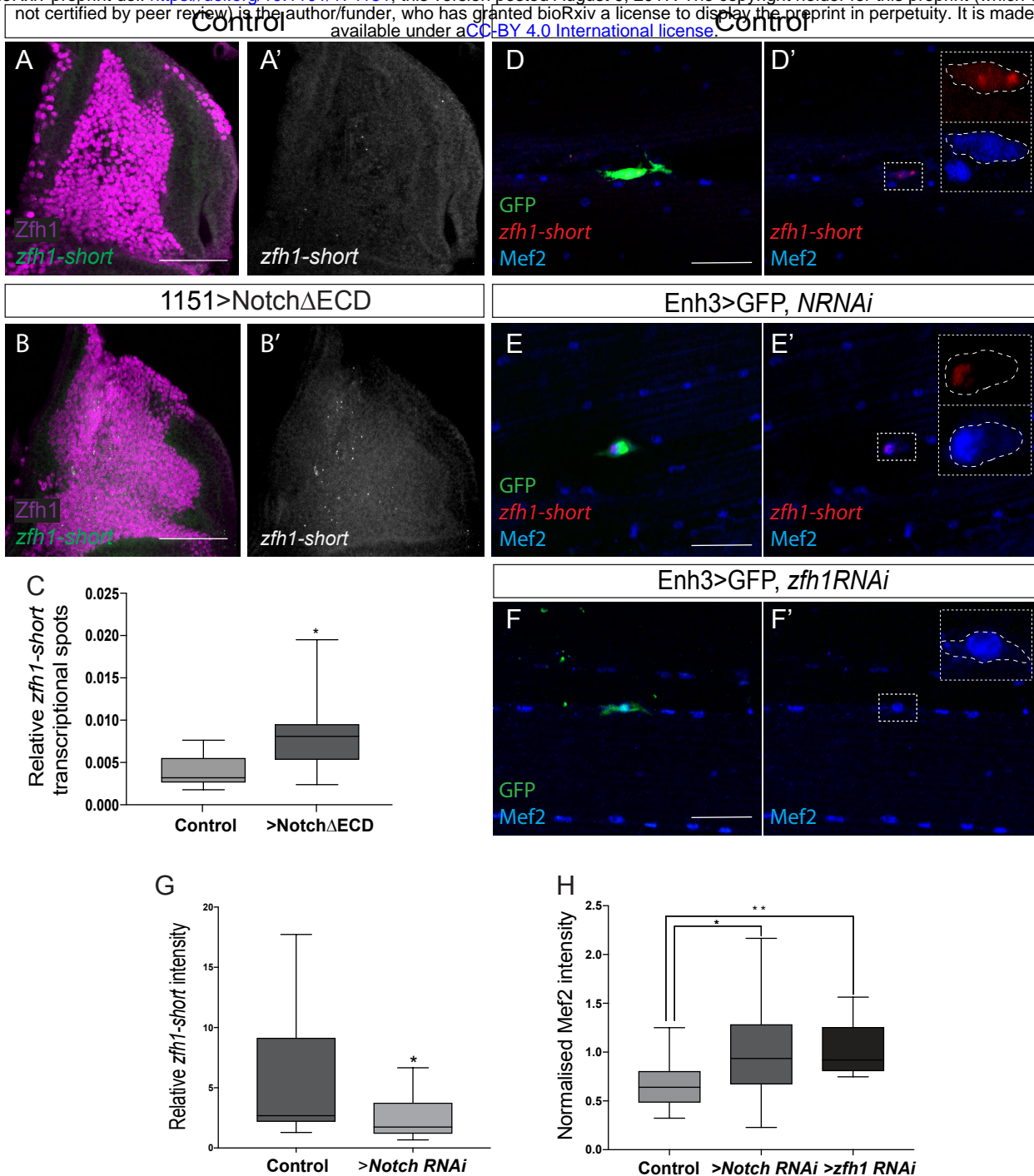


Figure 6. Notch is required to transcribe *zfh1-short* in the pMPs.

(A-C). Expression of an activated Notch (1151-Gal4>UAS-N Δ ECD) in MPs induces ectopic *zfh1-short* transcription. *In situ* hybridisation detecting *zfh1-short* (green) in MPs (Zfh1, purple) with wild type (A-A') or elevated Notch activity (B-B'). Scale bars: 50 μ M. (C). Quantification showing significant increase in nuclear puncta of *zfh1-short* upon Notch up regulation (* $p = 0.014$, $n = 10$, Student t-test). (D-E). Notch depletion leads to a severe decrease in *zfh1-short* (red) (D'-E' and G) in pMPs (green; *Enh3-Gal4*>UAS-*mCD8GFP*) and to an increase in Mef2 levels (F-F'). *Enh3-Gal4* was used to drive expression of control RNAi (D-D'), *Notch RNAi* (E-E'), or *zfh1 RNAi* (F-F') specifically in pMPs. Mef2 (blue) marks all muscle and pMP nuclei. Scale bars: 25 μ M. (G-H). Quantification of *zfh1-short* (G) and of Mef2 (H) in the indicated conditions, levels are significantly different (* $p = 0.0417$, $n = 14$ in G; * $p = 0.03$, $n = 13$ (*Notch RNAi*) and ** $p = 0.0029$, $n = 14$ (*Zfh1 RNAi*) in H).

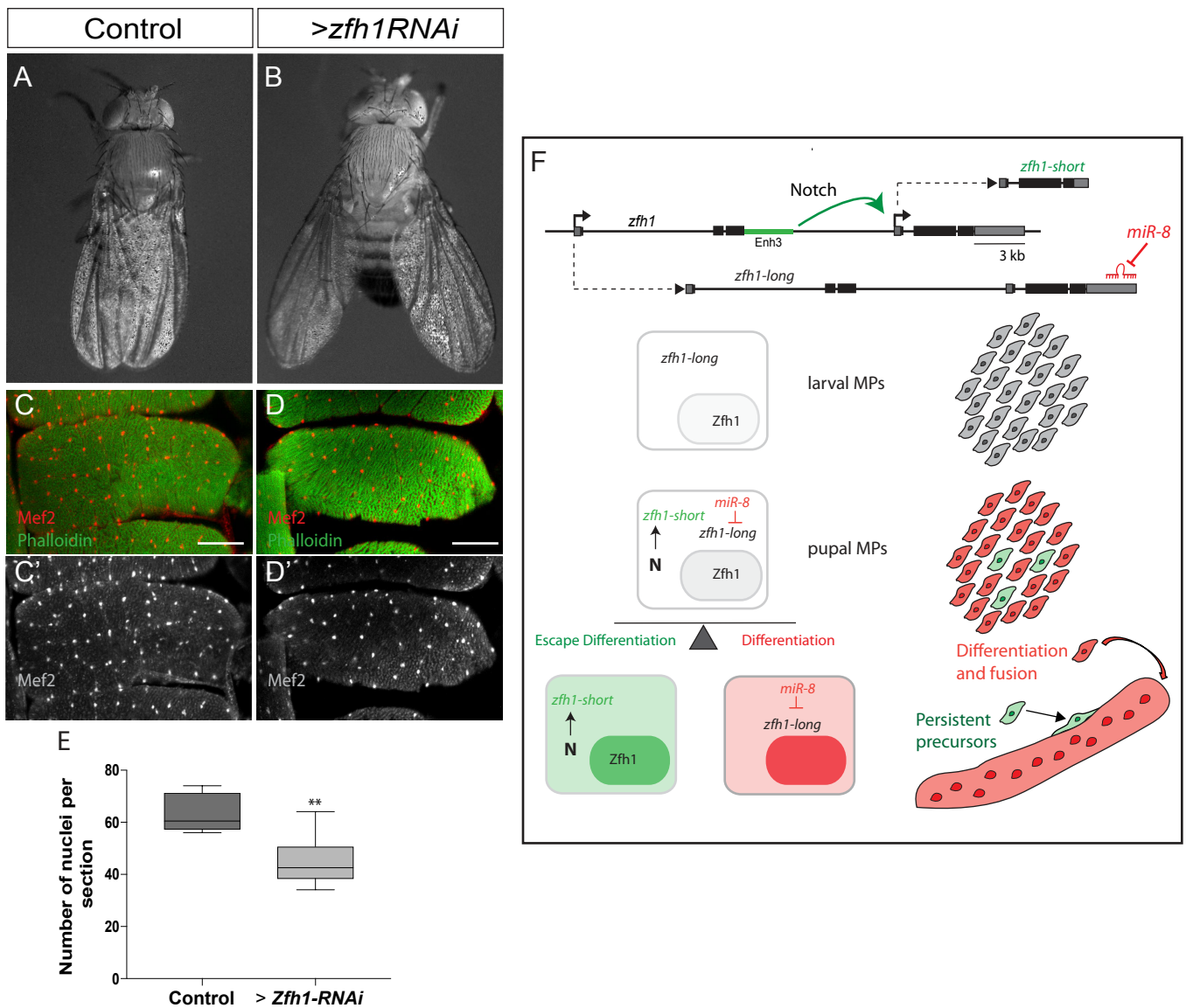


Figure 7. Zfh1 expression in pMPs is important to maintain muscle homeostasis.

(A-B). Prolonged *zfh1* depletion in pMPs leads to a “held out” wings posture; dorsal view of (A) control (*Enh3-Gal4>UAS-wRNAi; tubGal80ts*) and (B) *zfh1* depletion (*Enh3-Gal4>UAS-zfh1RNAi; tubGal80ts*) adult flies. (C-E). Fewer Mef2+ve nuclei are present in muscles when *zfh1* is depleted from pMPs. Transverse sections of DLM4 muscle stained with Phalloidin (green) and Mef2 (red, white) from the indicated genotypes. Scale bars: 50 μ m. (E) The number of nuclei per section in the

indicated conditions was significantly different. (** $p = 0.0013$, $n=10$, Student t-test). (F). Model summarizing the role of alternate *zfh1* isoforms in the maintenance of adult pMPs. *zfh1-long* (Grey) is expressed in all MPs at larval stage. Silencing of *zfh1-long* by *miR-8* (Red) facilitates the MPs differentiation. *zfh1-short* (Green) transcription is driven and maintained in pMPs by a Notch responsive element (*Enh3*, Green rectangle). Because *zfh1-short* is invisible to *miR-8*, Zfh1 protein is maintained in pMPs, enabling them to escape differentiation and persist as MPs in the adult.

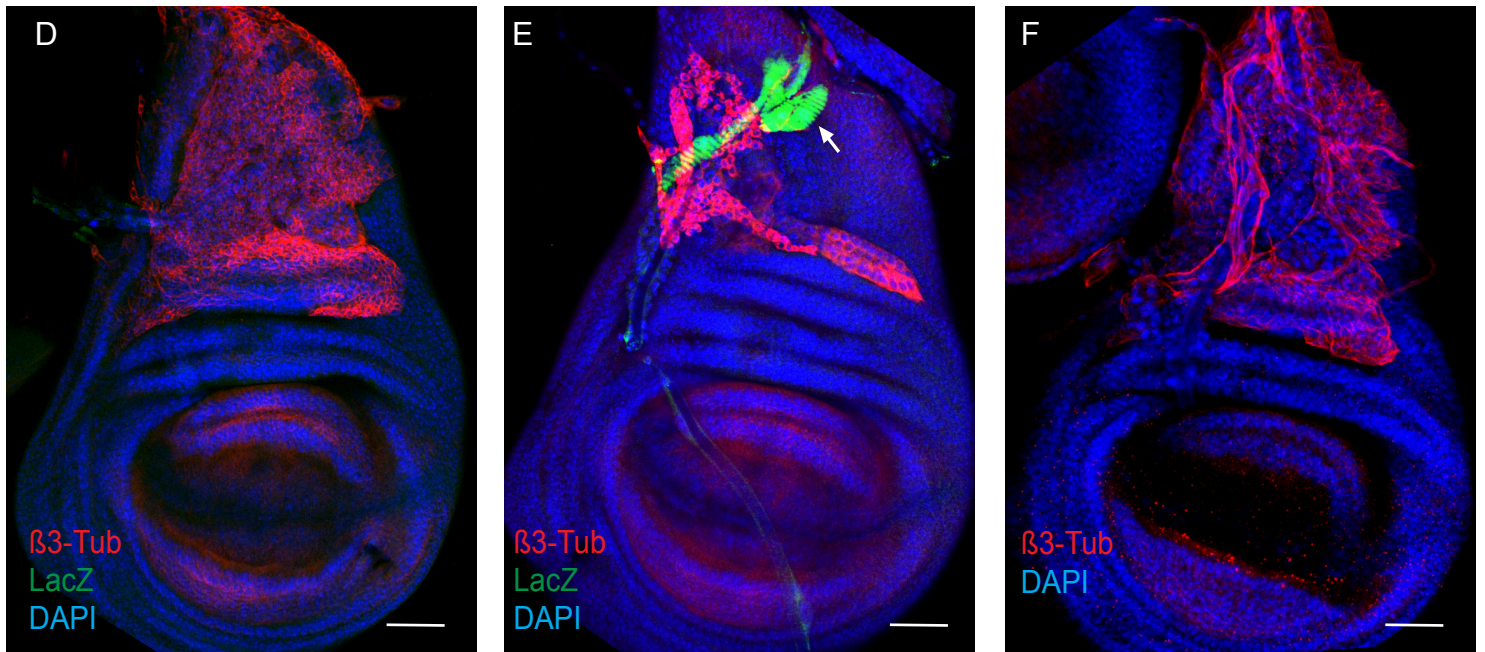
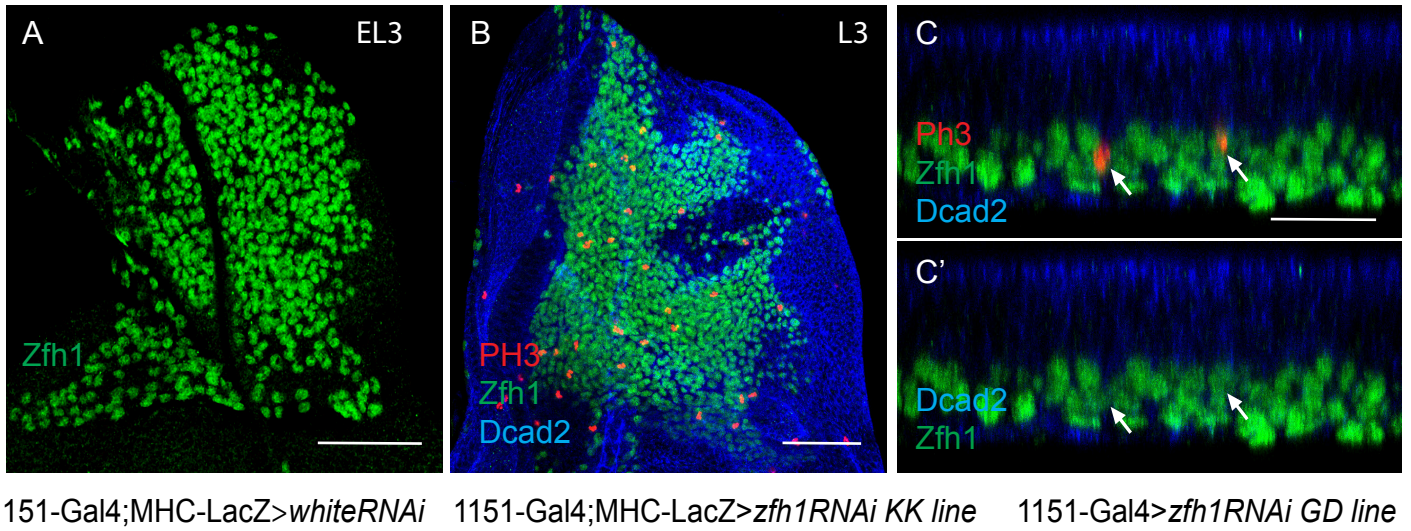


Figure supplement 1. A. Zfh1 (Green) expression in MPs associated with early third instar wing discs showing that at this stage Zfh1 is uniformly expressed in all the MPs. Scale bar : 50 μM. **B.** Third instar wing discs stained for Zfh1 (Green), PH3 (Red) and Dcad2 (Blue) revealing that some MPs are undertaking mitotic divisions. Scale bar: 50 μM. **(C-C')**. Optical section of image B showing active mitotic division of Zfh1 MPs in the most proximal layer to the disc epithelium (Arrows). Scale bar: 25 μM. **(D-F)**. β3-Tubulin (β3-Tub, red), LacZ (Green) and DAPI (Blue) expression in control (D, *1151-Gal4; mhc-lacZ > UAS-white-RNAi*) and *zfh1* down regulation (*1151-Gal4>UAS-zfh1-RNAi*) with two different RNAi transgenes, KK 103205 and GD42856, in E and F, respectively. Scale bars : 50 μM. **E.** Premature differentiation of MPs is observed using the KK103205 RNAi line comparing to the control (Arrow). **F.** Intermediate MPs differentiation phenotype is evident with the GD42856 RNAi transgene. MPs adopt an elongated morphology without expressing any muscle differentiation marker.

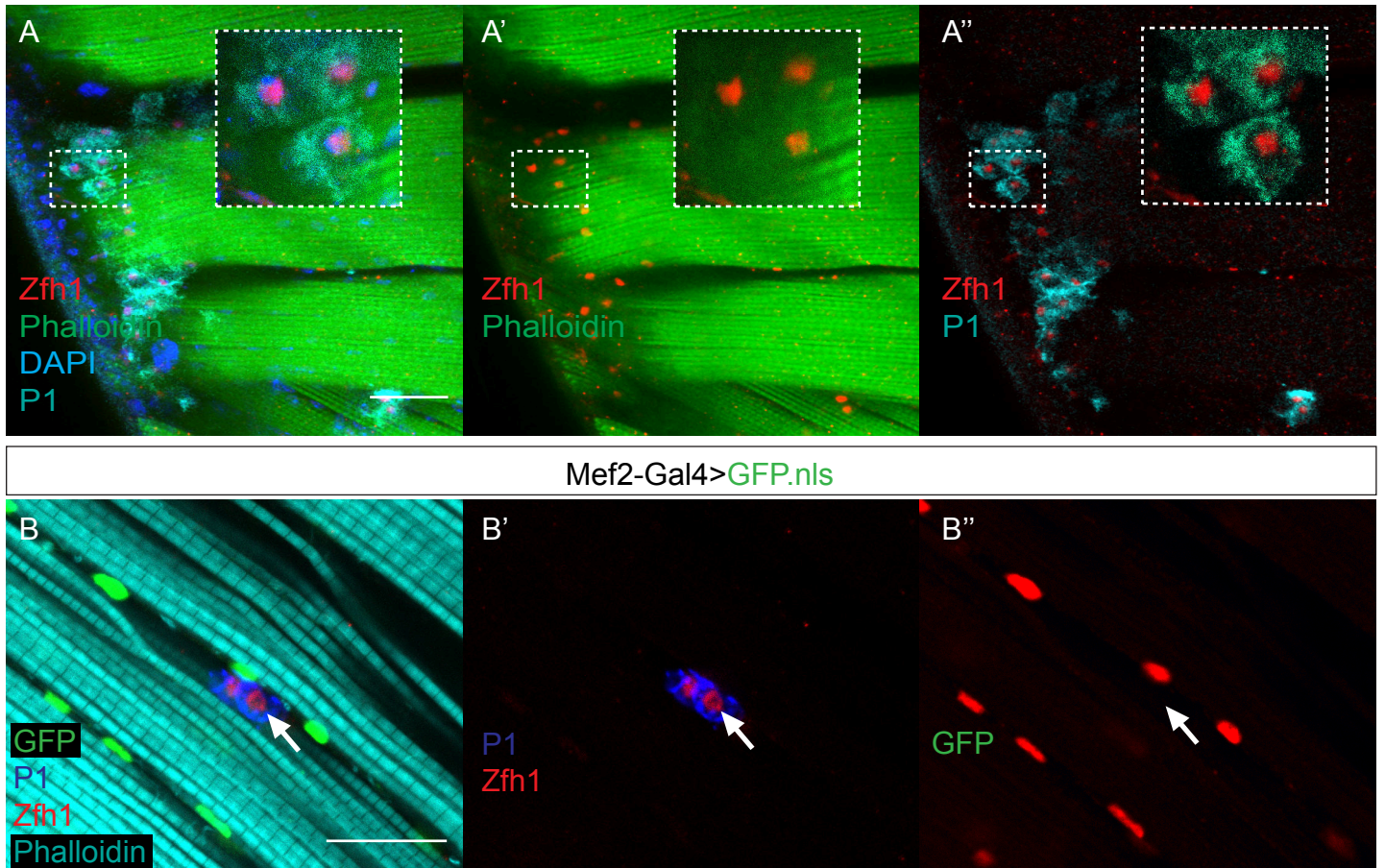


Figure supplement 2. A-A''. Wild type indirect flight muscles stained for P1 (Cyan), Zfh1 (Red), Phalloidin (Green) and DAPI (Blue). P1 expression indicates the presence of phagocytic immune cells, which are also positive for Zfh1. Insets: boxed regions magnified 4X. Scale bar: 50 μ M. **B-B''.** Indirect flight muscles from flies expressing *Mef2-Gal4>UAS-GFPnls* stained for GFP (Green), P1 (Blue), Zfh1 (Red) and Phalloidin (Cyan). The Zfh1 immune cells detected in the IFMs lack Mef2 expression (Arrows B-B''). Scale bar: 25 μ M.

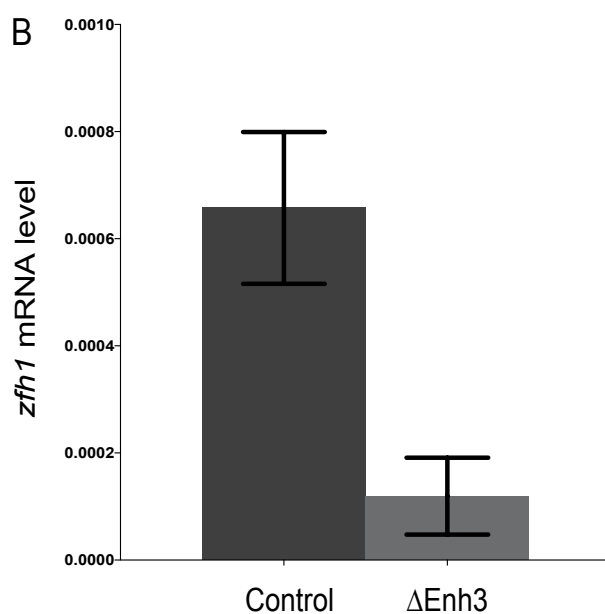
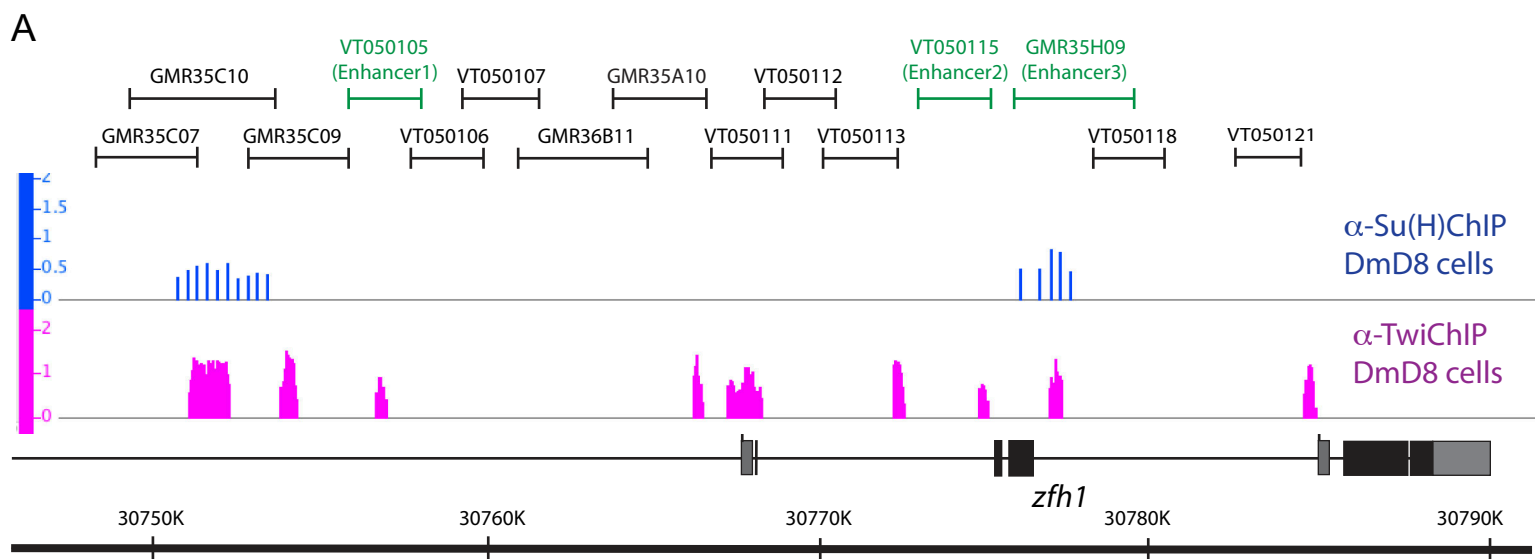


Figure supplement 3. A. Identification of active *zfh1* enhancers in MPs and pMPs. Chromosome 3R: 30,765,926-30,789,202 showing the *zfh1* genomic region with coding exons and untranslated regions represented in black and grey boxes, respectively. Arrows represent the transcription starts. Su(H) and Twi Chip enriched regions in DmD8 cells are represented in Blue and Magenta, respectively (Data from Bernard et al., 2010 (Chip Twi) and Krejci et al., 2009 (Chip Su(H))). Black lines represent all GMR and VT lines tested in our study. Green lines indicate the enhancers that are active in MPs *in vivo*. **B.** Effect of Enh3 Crisper deletion (Δ Enh3) on *zfh1* mRNA level in larval MPs as determined by quantitative RT-PCR. *zfh1* mRNA level is significantly decreased by Enh3 deletion.

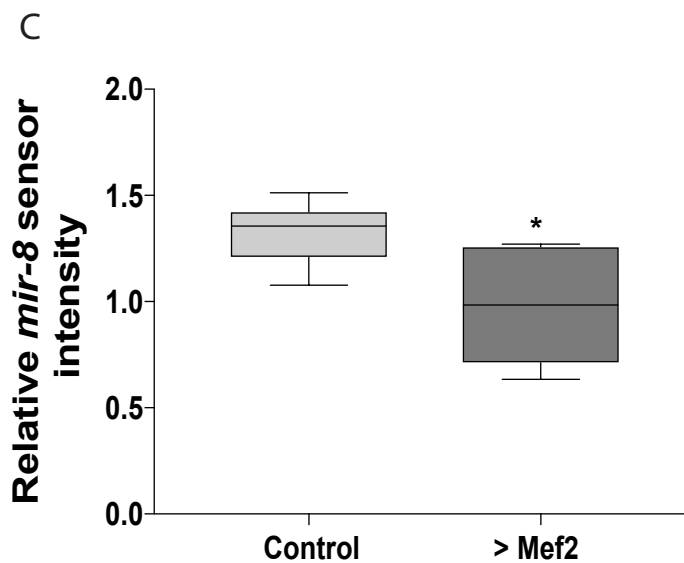
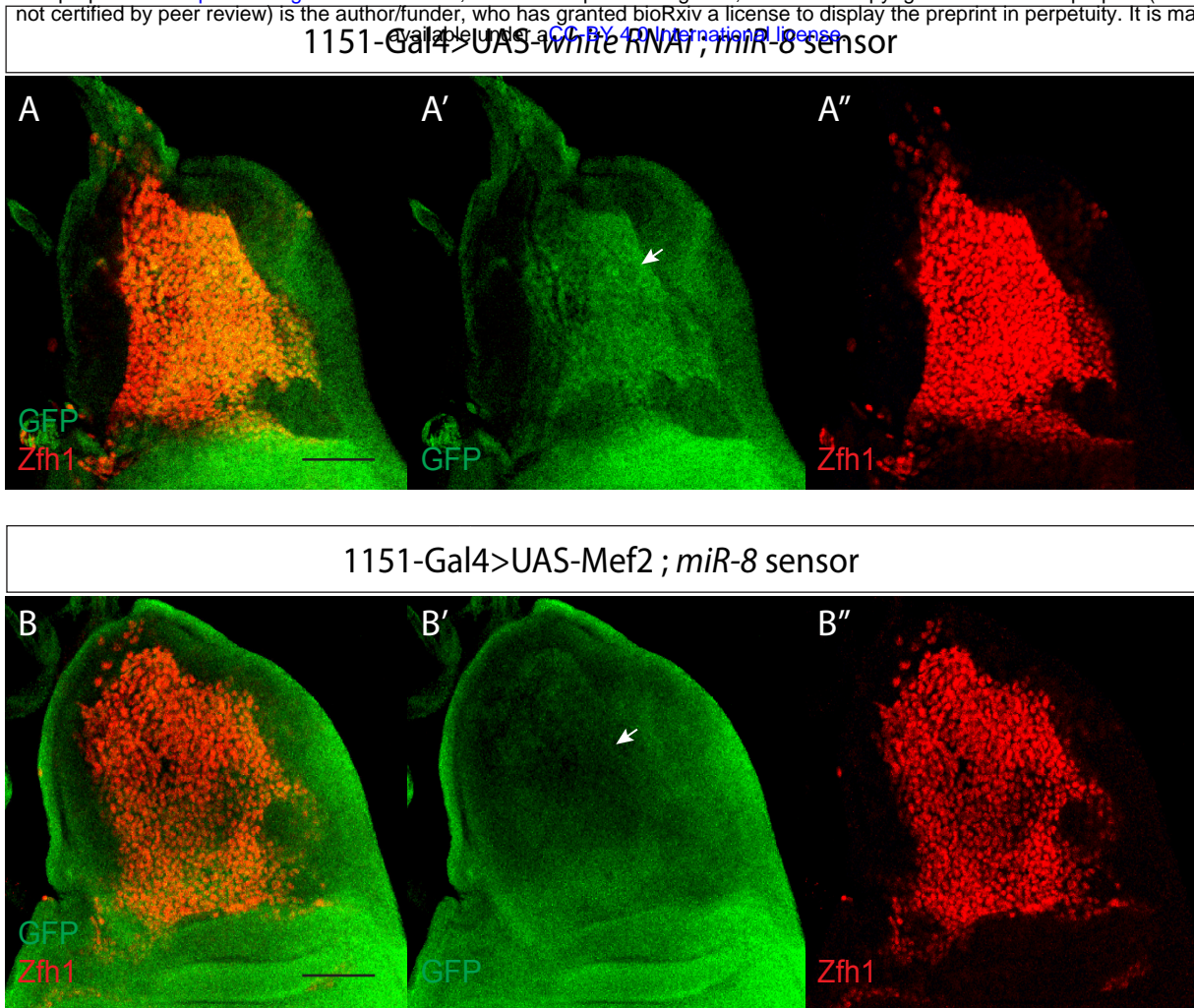


Figure supplement 4. *miR-8* responds to high level of Mef2. *miR-8* activity was detected using *miR-8-EGFP* sensor (Kennel et al., 2012). (A-B). Effect of Mef2 overexpression (1151-Gal4>UAS-Mef2) on *miR-8* sensor (Green) expression level in MPs. *miR-8* sensor expression in MPs is significantly reduced by Mef2 overexpression (Arrows in A' and B'). Zfh1 expression (Red) was used to visualise the MPs. (C). Quantification of *miR-8* Sensor intensity in the indicated conditions. (* $p = 0.0164$, $n = 8$). Scale bars = 50 μ M.

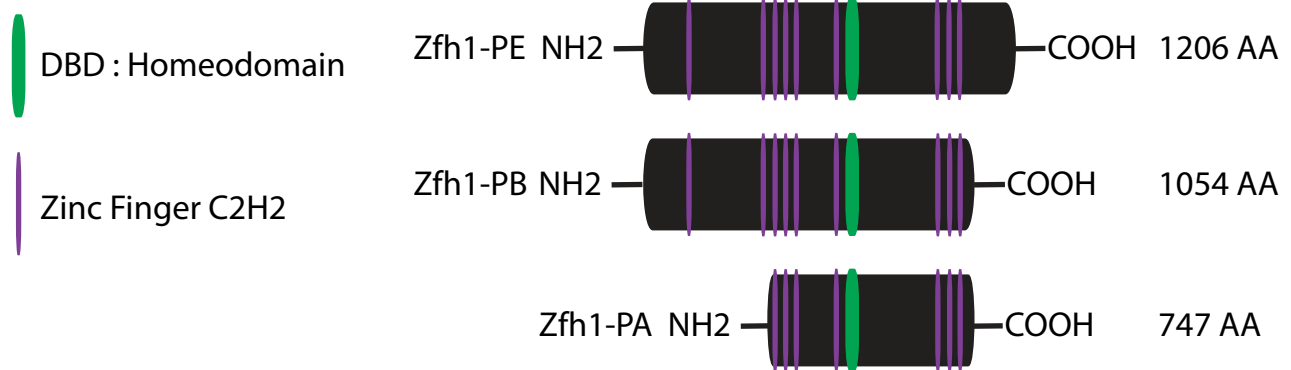


Figure supplement 5. Domain structure of *Drosophila* Zfh1 protein isoforms E, B and A. Magenta bars indicate the predicted zinc fingers, Green bar indicates the predicted homeodomain. All three protein-isoforms contain the core zinc finger and homeodomains needed for Zfh1 DNA-binding activity. Isoforms E and B contain two additional N-terminal zinc fingers (Postigo, et al., 1999).

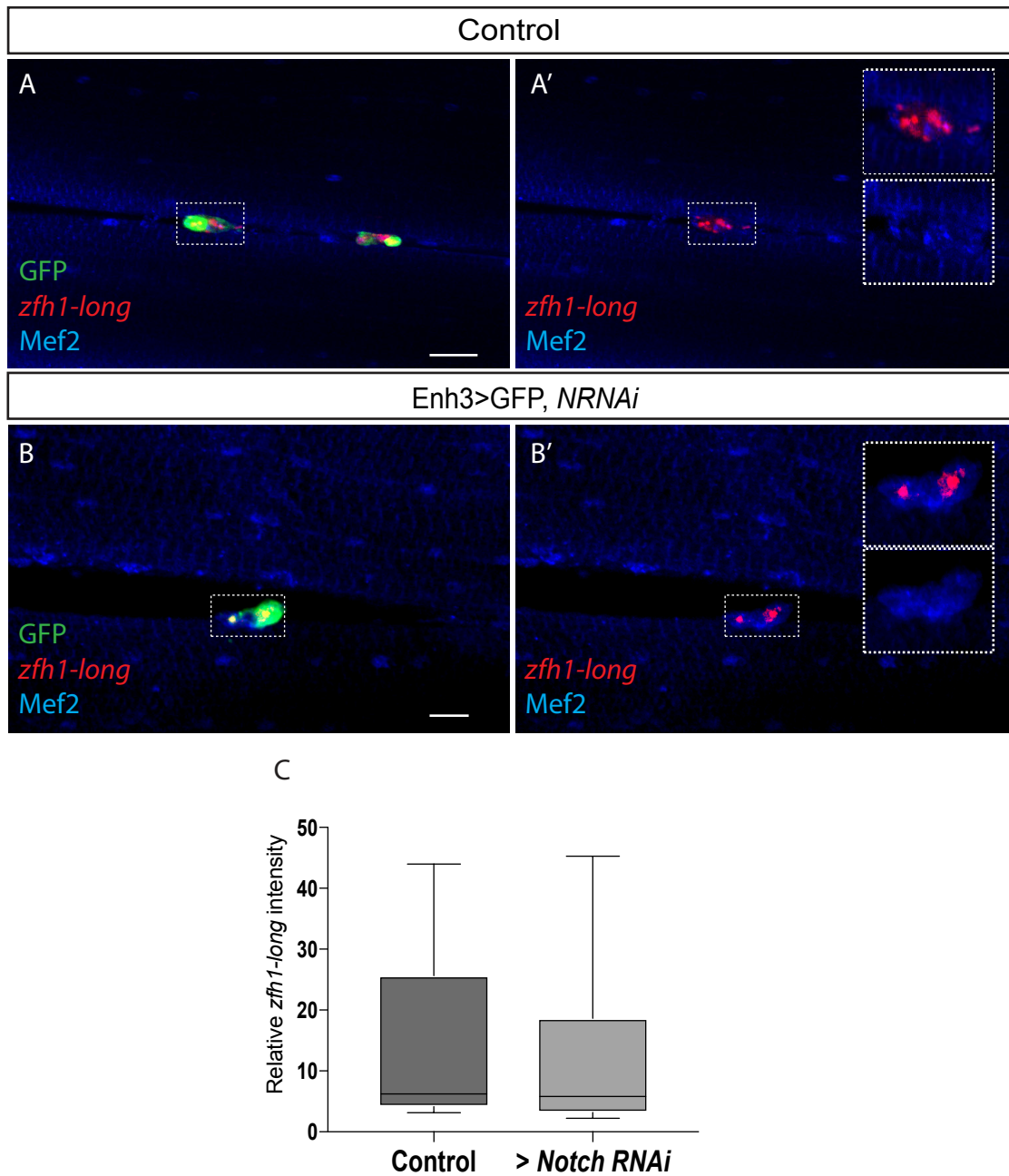


Figure supplement 6. Notch activity is not necessary for *zfh1-long* (red) transcription (A'-B' and C) in pMPs (green; *Enh3-Gal4>UAS-mCD8GFP*). *Enh3-Gal4* was used to drive expression of control RNAi (A-A'), *Notch* RNAi (B,B') specifically in pMPs. Mef2 (Blue) marks all muscle and pMP nuclei. Scale bars: 25 μ M. (C) Quantification of *zfh1-long* intensity in the indicated conditions, no significant difference was detected.